

Dual-Functional Nano-Photosensitizers: Eosin-Y Decorated Gold Nanorods for Plasmon-Enhanced Fluorescence and Singlet Oxygen Generation

Sravani Kaja, Ashin Varghese Mathews, and Amit Nag*

Department of Chemistry, Birla Institute of Technology and Science (BITS) Pilani,
Hyderabad Campus, Hyderabad-500078, India

* Email: amitnag@hyderabad.bits-pilani.ac.in

Table of contents:

1. Experimental section

1.1. Synthesis of Amine Functionalized SiNPs

1.2. Synthesis of SiNP-LBL NPs

1.3. Eosin Y Conjugation on SiNP-LBL NPs

1.4. COMSOL simulations

2. Sample preparation

2.1. Calibration Curve for Quantification of Conjugated Ey on NPs

2.2. Metal Enhanced Fluorescence (MEF) and Lifetime Studies

2.3. Singlet Oxygen Generation (SOG) Studies

2.4. Experimental method for detection of Scattering

Figure S1: Average size plots of GNRs

Table S1: LSPR band maxima, length, width and Aspect ratio of synthesized GNRs

Figure S2: Zeta potential measurements on GNRs

Figure S3: Zeta potential measurements on GNR 1a-1f

Figure S4: Zeta potential measurements on GNR 2a-2f

Figure S5: Zeta potential measurements on GNR 3a-3f

Figure S6: Zeta potential measurements on GNR 4a-4f

Figure S7: Zeta potential measurements on GNR 5a-5f

Figure S8: Zeta potential measurements on GNR 6a-6f

Figure S9: Extinction spectra of LBL assembled GNRs

Figure S10: FE-SEM of GNR 1a-1f

Figure S11: Average size plots of GNR 1a-1f

Figure S12: FE-SEM of GNR 2a-2f

Figure S13: Average size plots of GNR 2a-2f

Figure S14: FE-SEM of GNR 3a-3f

Figure S15: Average size plots of GNR 3a-3f

Figure S16: FE-SEM of GNR 4a-4f

Figure S17: Average size plots of GNR 4a-4f

Figure S18: FE-SEM of GNR 5a-5f

Figure S19: Average size plots of GNR 5a-5f

Figure S20: FE-SEM of GNR 6a-6f

Figure S21: Average size plots of GNR 6a-6f

Figure S22: plot showing increase in average layer thickness with number of layers

Figure S23: Extinction spectra of GNR-LBL-Ey

Figure S24: Extinction spectra of supernatant after GNR-LBL-Ey conjugation

Figure S25: Photograph of supernatant of samples after GNR-LBL-Ey conjugation under UV light

Figure S26: Zeta potential change on LBL GNR after Ey conjugation

Figure S27: Calibration curve of Ey

Calculation S1: Calculation of Number density of GNRs and SiNPs

Figure S28: MEF studies on GNR-LBL-Ey

Figure S29: Characterization of SiNPs

Figure S30: MEF EF of Ey adsorbed on LBL-GNR

Figure S31: Life time studies on GNR-LBL-Ey

Table S2: Lifetime studies on GNR 1a-1f

Table S3: Lifetime studies on GNR 2a-2f

Table S4: Lifetime studies on GNR 3a-3f

Table S5: Lifetime studies on GNR 4a-4f

Table S6: Lifetime studies on GNR 5a-5f

Table S7: Lifetime studies on GNR 6a-6f

Figure S32: Blank studies for SOG

Figure S33: SOG studies on GNR 1 to 6 in presence and absence of PS

Figure S34: SOG studies on GNR 1a-1f

Figure S35: SOG studies on GNR 2a-2f

Figure S36: SOG studies on GNR 3a-3f

Figure S37: SOG studies on GNR 4a-4f

Figure S38: SOG studies on GNR 5a-5f

Figure S39: SOG studies on GNR 6a-6f

Figures S40: $\ln(A_0/A)$ plots for obtained SOG data

Figure S41: EF SOG plots for GNR-LBL-Ey

Figure S42: COMSOL studies on GNR 1-6 without any coating

Figure S43: COMSOL studies on GNR 4a-4f

Figure S44: Decay length plot of GNR 1d-6d

Figure S45: 1D line plot showing the normalized electric field damping as a function of distance for bare GNRs

Figure S46: Experimental scattering of GNR 4a-4f

1. Experimental section:

1.1. Synthesis of Amine Functionalized SiNPs

Modified Stober's method was used for the one step synthesis of SiNPs.¹ This involves the simultaneous hydrolysis of TEOS and APTES in the presence of NH₄OH and Ethanol. For the synthesis, typically a solution containing 3 mL of aqueous Ammonia solution, 3 mL of distilled water, and 44 mL of ethanol was added to a beaker and stirred at 1500 rpm at room temperature. To this solution a solution containing 45 mL of ethanol and 5 mL TEOS was added quickly and the solution was then allowed to react for 2 hours at room temperature on a magnetic stirrer. It was later centrifuged and the pellet was washed with water and ethanol to remove unreacted precursor and finally dried in an oven at 60 °C and the obtained powder is dispersed at 2 mg/mL concentration for further studies.

1.2. Synthesis of SiNP-LBL NPs

LBL assembly on SiNPs was carried out in a similar way as that of GNRs. SiNPs synthesized were first coated with PSS layer, then followed by PAH. This process was repeated three times and the obtained SiNPs were purified by centrifugation and are labelled as SiNP-LBL a to SiNPs-LBL f.

1.3. Eosin Y Conjugation on SiNP-LBL NPs

The conjugation was carried out in a similar manner as that of GNRs. To SiNP solution 10 µL of 10 mM Ey solution in ethanol was added and the solution was stirred at 600 rpm for 3 hours using a magnetic stirrer. Then the solution was centrifuged and the pellet and supernatant were separated. The pellet was further redispersed in water and centrifuged again. This washing process is repeated for at least 3 times to remove excess unbound Ey.

1.4. COMSOL SIMULATION

COMSOL simulation was done using the electromagnetic wave, frequency domain module (emw). For this GNR was placed in an air box and all the simulations were carried out using an incident wavelength of 519 nm and the scatter field of the GNR is observed. The propagation of the incident wave is along the x-axis with an electric field strength of 1V/m. The mesh size is set to predefined "Finer" and the properties of the materials used are obtained from the COMSOL material library. The three materials used are Gold [Au (Gold) (Windt et al. 1988: n, k 0.0024-0.1216 µm)], Water [liquid], and Silica [SiO₂ (fused quartz) [solid, NIST SRM 739

- Type I]]. The parameters such as electric conductivity, relative permeability, and permittivity were added as the external parameters of the material. In order to study the scattered field after the incident electromagnetic wave interacts with the GNR, we defined a boundary condition around the GNR as a cube that has its length of one side set as 400 nm. A two-dimensional electric field map is obtained from the scattered field.

The values that are externally fed in to simulation were: Relative permeability for gold: 0.999998; Electrical conductivity for gold: 4.11e7 S/m; Relative permeability for water: 0.9999992; The relative permittivity of SiO₂: 3.9; Relative permeability for SiO₂: 0.9999704; Electrical conductivity for water: 5.5e-6 S/m.

Theoretical electrical field enhancement factor was calculated as the second power of the electric field that is experienced by the nanorods. For this simulation, the EF is calculated using the formula,

$$EF = [E]^2 = \left[\frac{(E_{max} - E_{min})}{E_{applied}} \right]^2$$

The equation represents how to calculate the electrical field, which forms as the response to the EM waves interacting with the SiO₂ coated gold nanorods. Where, E_{max} = maximum electric field experienced by the GNR; E_{min} = minimum electric field experienced by the GNR and E_{applied} = applied electric field to the system along x axis (1V/m).

2. Sample preparation:

2.1. Calibration Curve for Quantification of Conjugated Ey on NPs

For all our conjugation experiments, we have used 10 µL of 10 mM Ey solution to 10 mL of GNR solution. It means the final added concentration of Ey in each solution is 10 µM. Keeping this in mind we have made a calibration curve using UV-Vis spectrophotometer in the range of 0.1 µM to 10 µM. we recorded the absorbance of Ey in all these concentration range and the OD values are noted. Then after conjugation, we recorded the absorbance of collected supernatant and the obtained pellet and then quantified the amount of Ey conjugated on GNRs.

2.2. Metal Enhanced Fluorescence (MEF) and Lifetime Studies

Before starting the experiment, all the Ey conjugated NRs solution and SiNP-LBL-Ey solutions was adjusted to same OD value to make sure that the concentration of Ey was same in all the samples. For all the fluorescence measurements, the samples were excited at 519 nm and the

emission was collected from 529 to 800 nm range. The excitation and emission slits were kept at 5 nm and the PMT voltage was set to 400. We have chosen SiNP-LBL-Ey as the appropriate blank to compare the result. The MEF Enhancement Factor (EF_{MEF}) was calculated as the ratio of fluorescence intensity (FI) of Ey in presence of GNRs to Fluorescence intensity of Ey in presence of SiNPs as following.

$$EF_{MEF} = \frac{FI_{GNR-LBL-Ey}}{FI_{SiNP-LBL-Ey}}$$

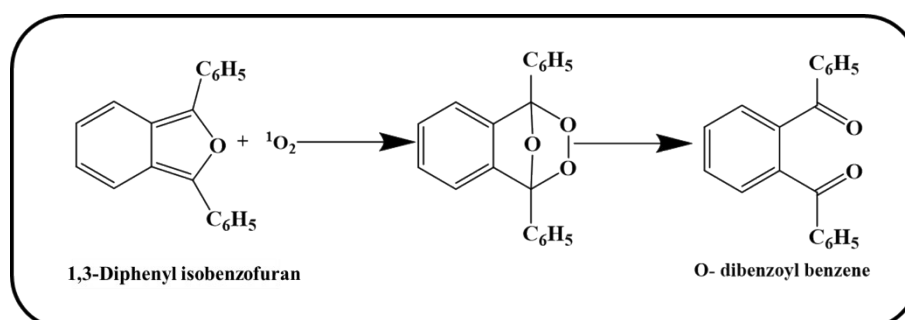
For excited state lifetime measurements, 510 nm LED was used as source and bandpass 4 nm, peak preset 10000 counts. All these parameters were kept constant throughout the entire experiment. Instrument response function (IRF) was done using LUDOX a colloidal SiNP solution and the emission wavelength was set to the wavelength of LED used. For sample, the emission wavelength was set as 540 nm and the obtained data is fitted using a tri exponential model and the average lifetimes were calculated using the formula:

$$\tau_{Avg} = \frac{\sum \alpha_i \tau_i^2}{\sum \alpha_i \tau_i}$$

Where, τ_i is the lifetime of a component, α_i is considered as the contribution of that particular component and τ_{avg} is the average lifetime.

2.3. Singlet Oxygen Generation (SOG) Studies

1,3-diphenylisobenzofuran (DPBF) was used as a probe to indirectly monitor the production of 1O_2 by the Ey conjugated GNRs. On irradiation with light, DPBF undergoes a 1,4-cycloaddition to form Ortho dibenzoyl benzene which has less absorbance compared to the parent compound due to less conjugation as shown in the figure below. This absorbance loss at 420 nm due to chemical trapping was exploited further to study the rate of production of Reactive oxygen species (ROS) by the GNR-LBL-Ey.



Scheme 1: Representation of Cycloaddition of DPBF in the presence of singlet oxygen.

Initially we prepared a stock of 0.1 mM DPBF in ethanol and later it was subsequently diluted in GNR solutions in water. For this experiment, we took 200 μL of 0.1 mM DPBF and added to 1.8 mL of diluted GNR-LBL-Ey solutions and irradiated it using a white light source with a power density of 35 mW/cm^2 . The decrease in absorbance of DPBF at 420 nm was measured at every 2 s for 30 s using a UV-Visible spectrophotometer. Later, the decay rate of the photosensitized process was determined by plotting the natural logarithm values of DPBF absorption at 420 nm against the irradiation time. These data points were then fitted to a first-order linear least-squares model and the slopes were noted. SiNP-LBL-Ey hybrids were used as a control sample to calculate the enhancement factor for the metal enhanced singlet oxygen generation (MESOG) as SiNPs are devoid of any plasmonic behaviour. The SOG EF was calculated as the ratio of slopes (K) of DPBF degradation in the GNR-LBL-Ey to SiNP-LBL-Ey as following.

$$EF_{SOG} = \frac{K_{GNR-LBL-Ey}}{K_{SiNP-LBL-Ey}}$$

Separate experiments were performed to confirm the presence of $^1\text{O}_2$ in the reaction mixture by adding a spin trapping probe 0.1 mM DMPO along with the addition of DPBF and irradiated with light. DMPO selectively binds to hydroxyl and superoxide radicals but not with $^1\text{O}_2$. Additionally, sodium azide (5 mg/mL) was introduced to the GNR-LBL-Ey solution in another experiment along with DPBF to validate the involvement of singlet oxygen ($^1\text{O}_2$) as the ROS. Measurements of absorbance values on irradiation of light in either case sheds some light on the ROS generated in the experiment.

2.4. Experimental method for detection of Scattering

The extinction of GNRs is the sum of scattering and absorption, and the scattering component can be determined experimentally using a integrated sphere.^{2,3} When an electromagnetic radiation (I_0) is incident on NP solution, several phenomena take place such as transmittance (I_T), scattering (I_S), absorption (I_A) and reflectance of light (I_R) from cuvette walls. The light reflectance from the cuvette walls is very negligible and can be ignored.

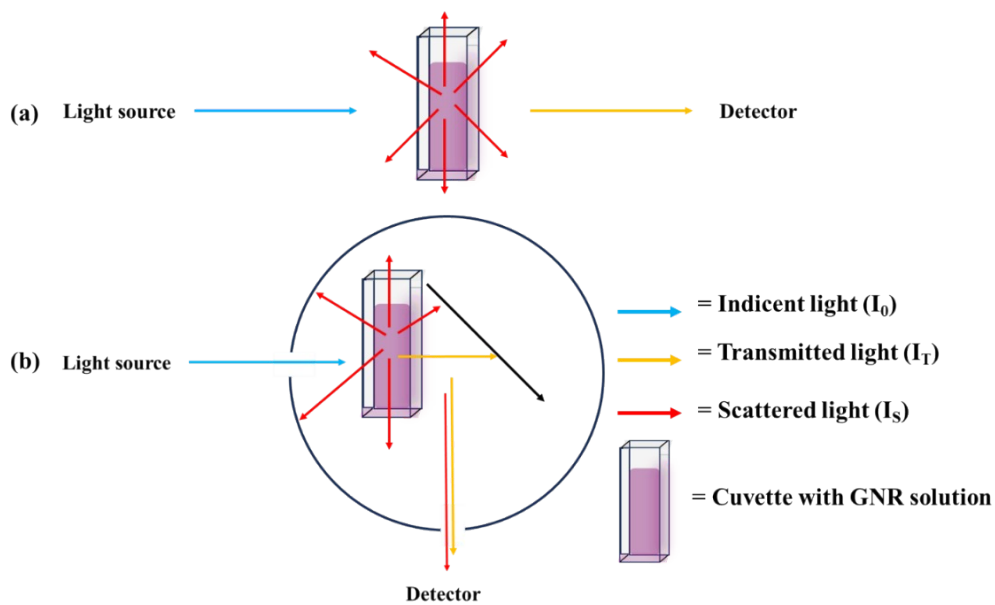
$$I_0 = I_A + I_T + I_S + I_R$$

$$I_0 = I_A + I_T + I_S \text{ (because } I_R \ll \ll I_0 \text{)}$$

While using a UV-Visible spectrophotometer, the light reaching the detector is dominated by transmittance and obtained spectra is a combination of light lost due to samples absorption and scattering. on the contrary while using an emission spectrometer coupled with an integrating sphere and placing the sample in it results in the detection of light from scattering and transmittance components implying that the light lost is mainly due to samples absorbance.

$$T_{UV-Vis} = I_T/I_0$$

$$T_{Integrating\ sphere} = (I_T+I_S)/I_0$$



Scheme 2: A pictorial representation of how extinction and scattering of samples was measured and (a) is the UV-Visible spectrophotometer used to collect the extinction of samples and (b) is the emission spectrophotometer coupled with an integrating sphere, used to measure scattering component.

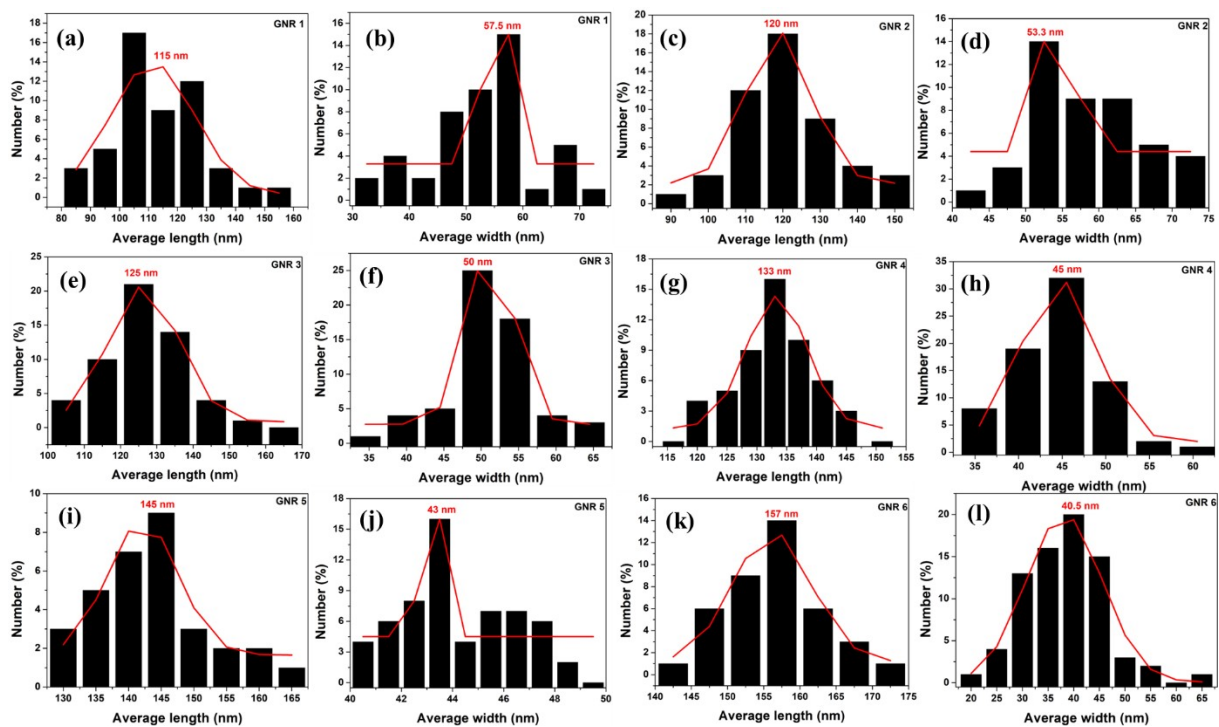


Figure S1: Average size plots of (a, b) GNR 1, (c, d) GNR 2, (e, f) GNR 3, (g, h) GNR 4, (i, j) GNR 5, and (k, l) GNR 6

Table S1: LSPR band maxima, length, width and Aspect ratio of synthesized GNRs

S.No.	Length (nm)	Width (nm)	AR	LSPR
1	115 ± 3.2	57.5 ± 2.1	2 ± 0.3	699
2	120 ± 2.3	53.3 ± 0.9	2.25 ± 0.7	716
3	125 ± 2.1	50 ± 1.9	2.5 ± 0.3	728
4	133 ± 4.7	45 ± 1.2	2.95 ± 0.8	751
5	145 ± 3.1	43 ± 1.7	3.37 ± 0.5	774
6	157 ± 4.6	40.5 ± 1.8	3.8 ± 0.9	828

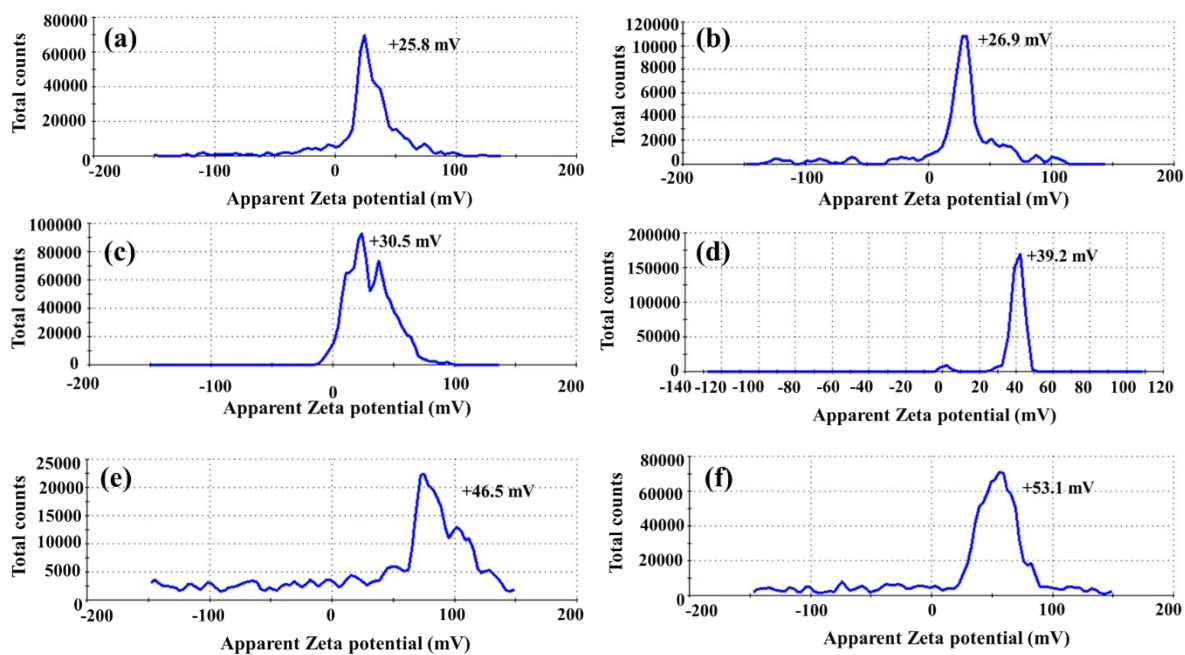


Figure S2: Zeta plots of (a) GNR 1, (b) GNR 2, (c) GNR 3, (d) GNR 4, (e) GNR 5, and (f) GNR 6

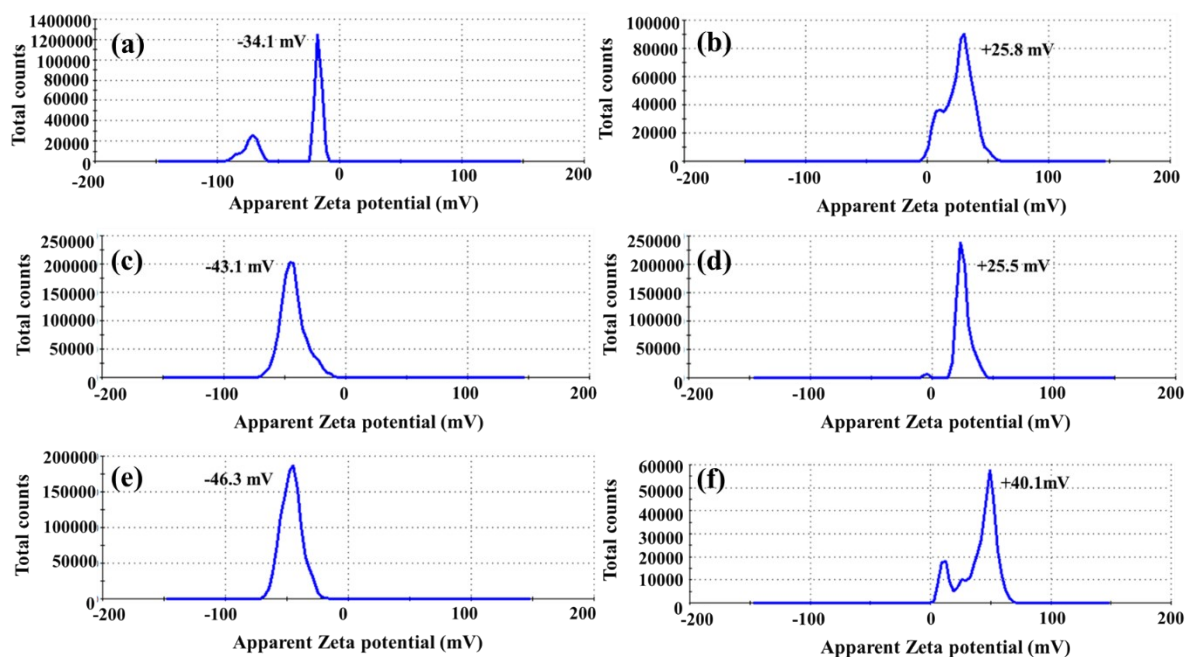


Figure S3: Zeta plots of GNR 1 with different LBL assemblies (a) GNR 1a, (b) GNR 1b, (c) GNR 1c, (d) GNR 1d, (e) GNR 1e, and (f) GNR 1f

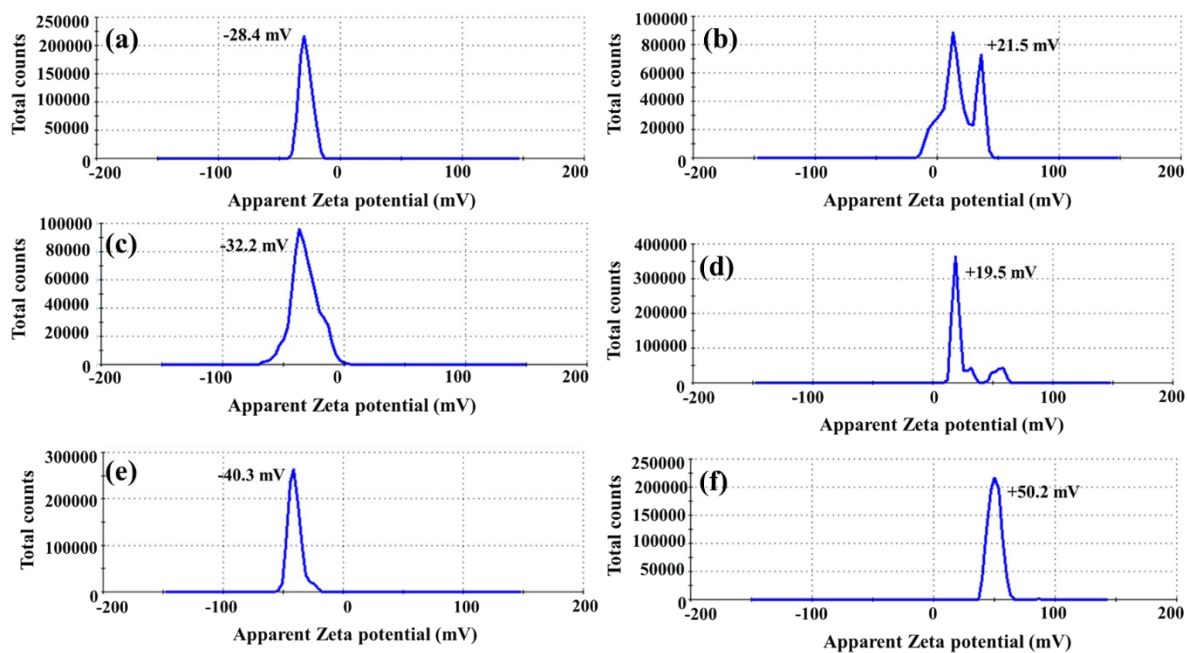


Figure S4: Zeta plots of GNR 2 with different LBL assemblies (a) GNR 2a, (b) GNR 2b, (c) GNR 2c, (d) GNR 2d, (e) GNR 2e, and (f) GNR 2f

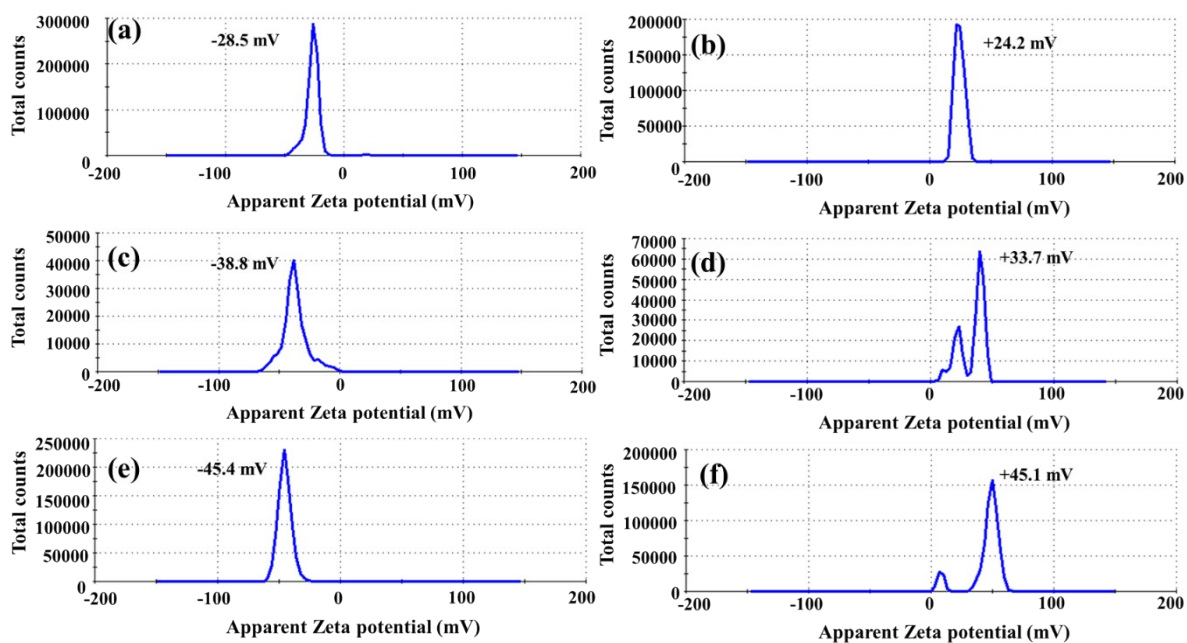


Figure S5: Zeta plots of GNR 3 with different LBL assemblies (a) GNR 3a, (b) GNR 3b, (c) GNR 3c, (d) GNR 3d, (e) GNR 3e, and (f) GNR 3f

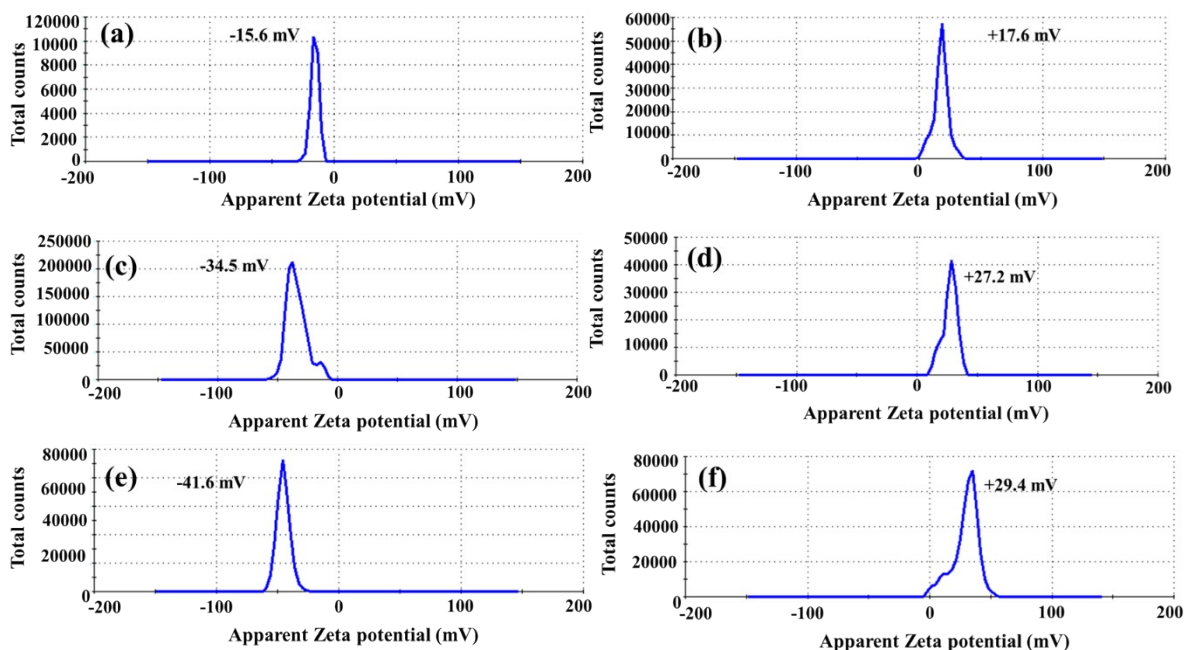


Figure S6: Zeta plots of GNR 4 with different LBL A assemblies (a) GNR 4a, (b) GNR 4b, (c) GNR 4c, (d) GNR 4d, (e) GNR 4e, and (f) GNR 4f

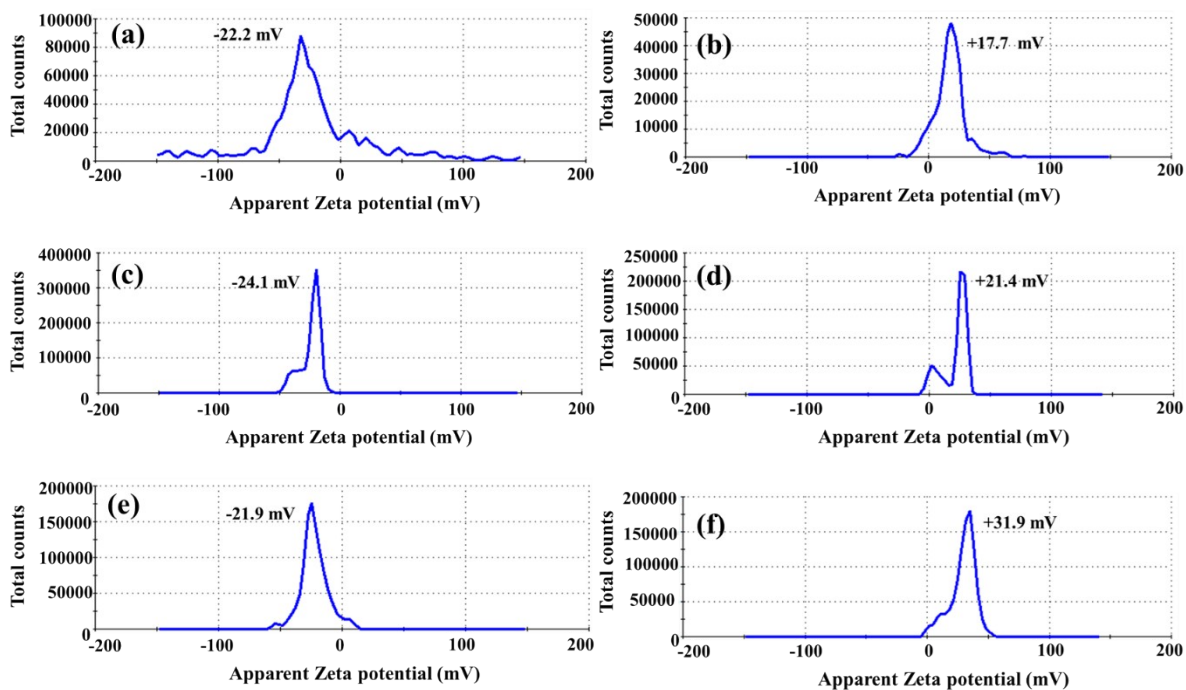


Figure S7: Zeta plots of GNR 5 with different LBL assemblies (a) GNR 5a, (b) GNR 5b, (c) GNR 5c, (d) GNR 5d, (e) GNR 5e, and (f) GNR 5f

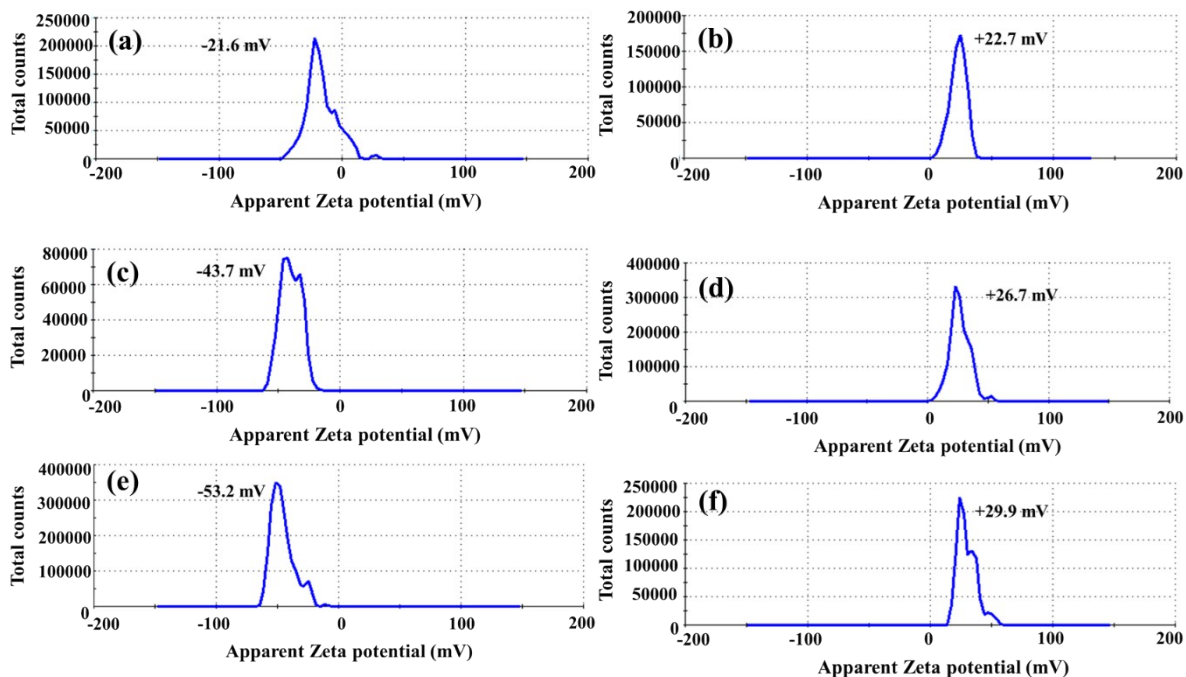


Figure S8: Zeta plots of GNR 6 with different LBL assemblies (a) GNR 6a, (b) GNR 6b, (c) GNR 6c, (d) GNR 6d, (e) GNR 6e, and (f) GNR 6f

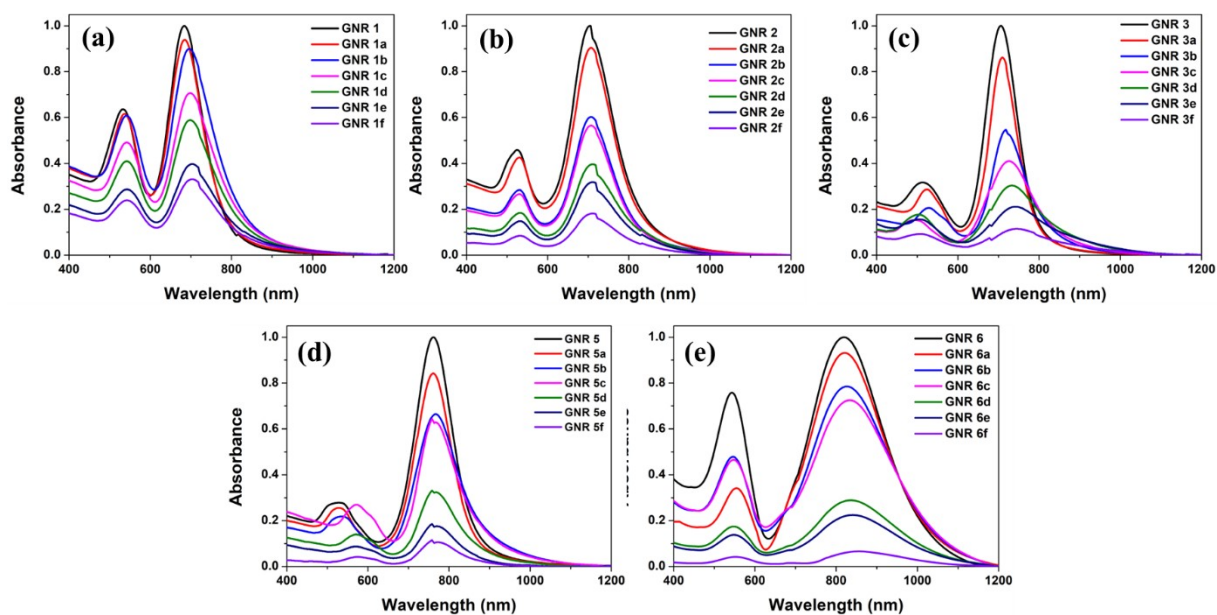


Figure S9: extinction spectra of (a) GNR 1a-1f, (b) GNR 2a-2f, (c) GNR 3a-3f, (d) GNR 5a-5f, and (e) GNR 6a-6f

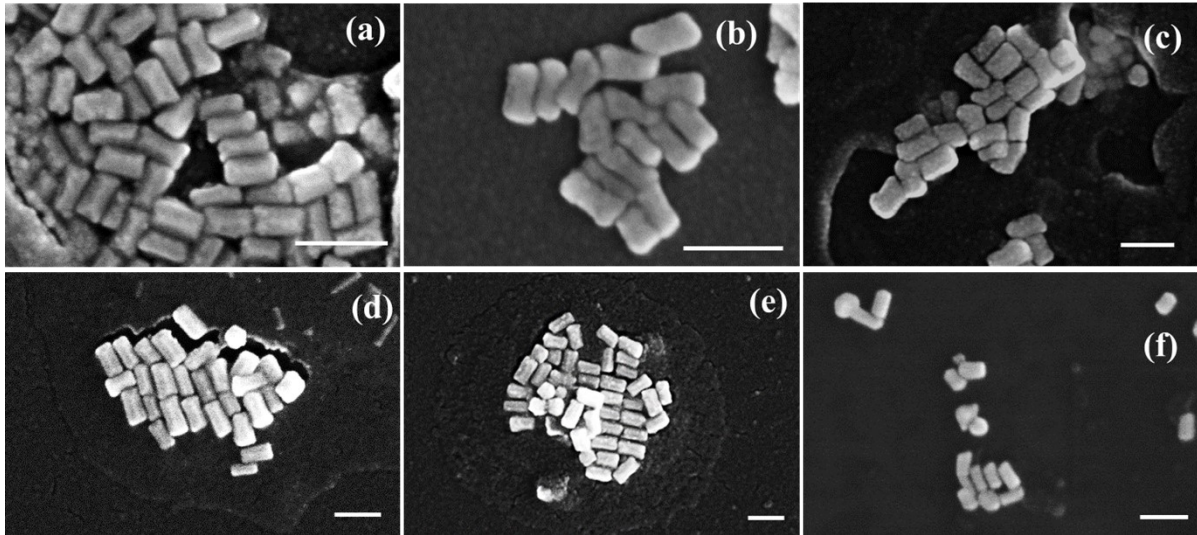


Figure S10: FE-SEM images of GNR 1 with different LBL assemblies (a) GNR 1a, (b) GNR 1b, (c) GNR 1c, (d) GNR 1d, (e) GNR 1e, and (f) GNR 1f and the scale bar is 200 nm

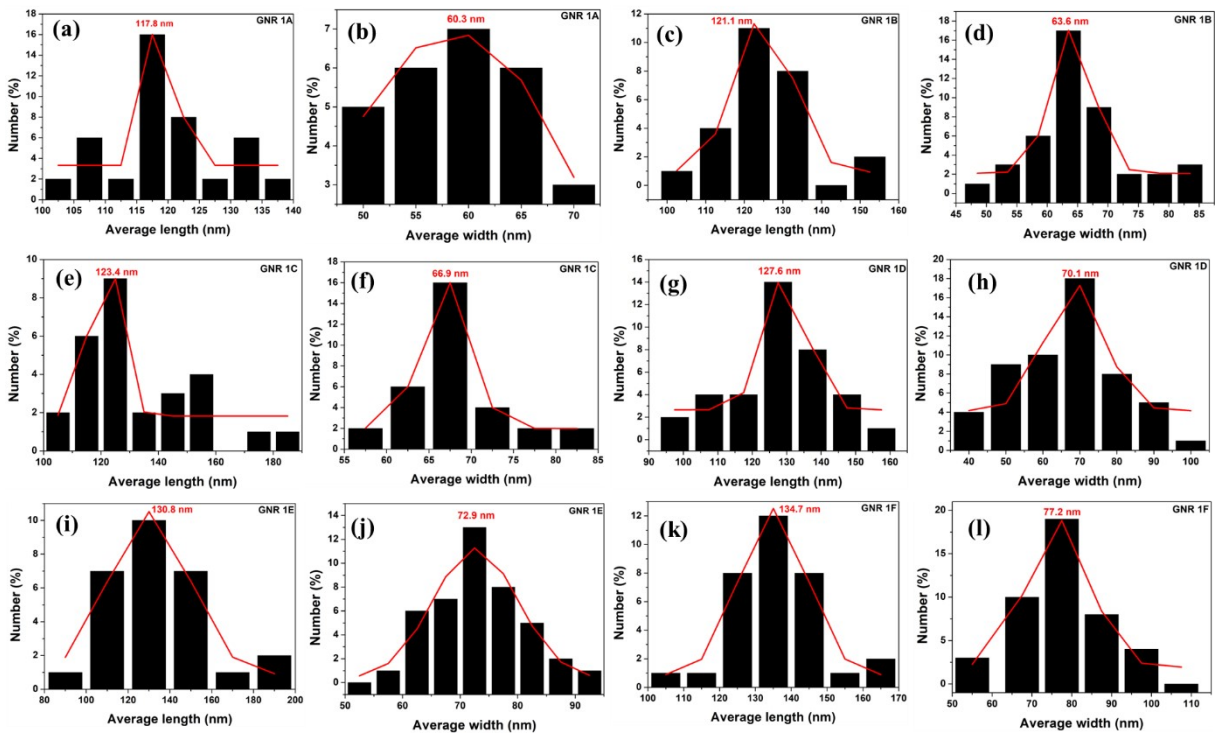


Figure S11: Average size plots of (a, b) GNR 1a, (c, d) GNR 1b, (e, f) GNR 1c, (g, h) GNR 1d, (i, j) GNR 1e, and (k, l) GNR 1f

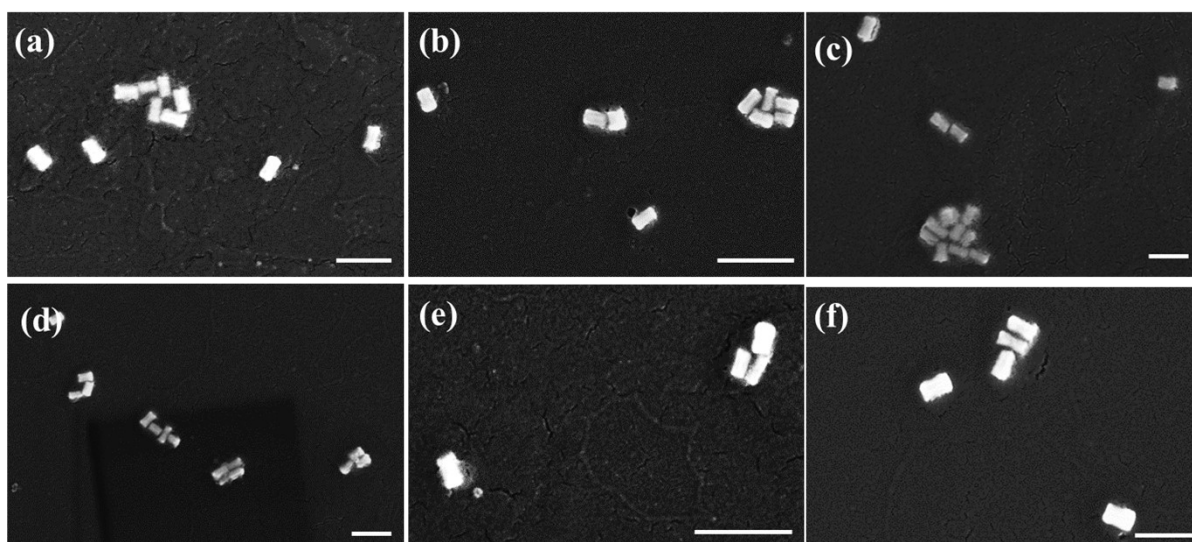


Figure S12: FE-SEM images of GNR 2 with different LBL assemblies (a) GNR 2a, (b) GNR 2b, (c) GNR 2c, (d) GNR 2d, (e) GNR 2e, and (f) GNR 2f and the scale bar is 200 nm

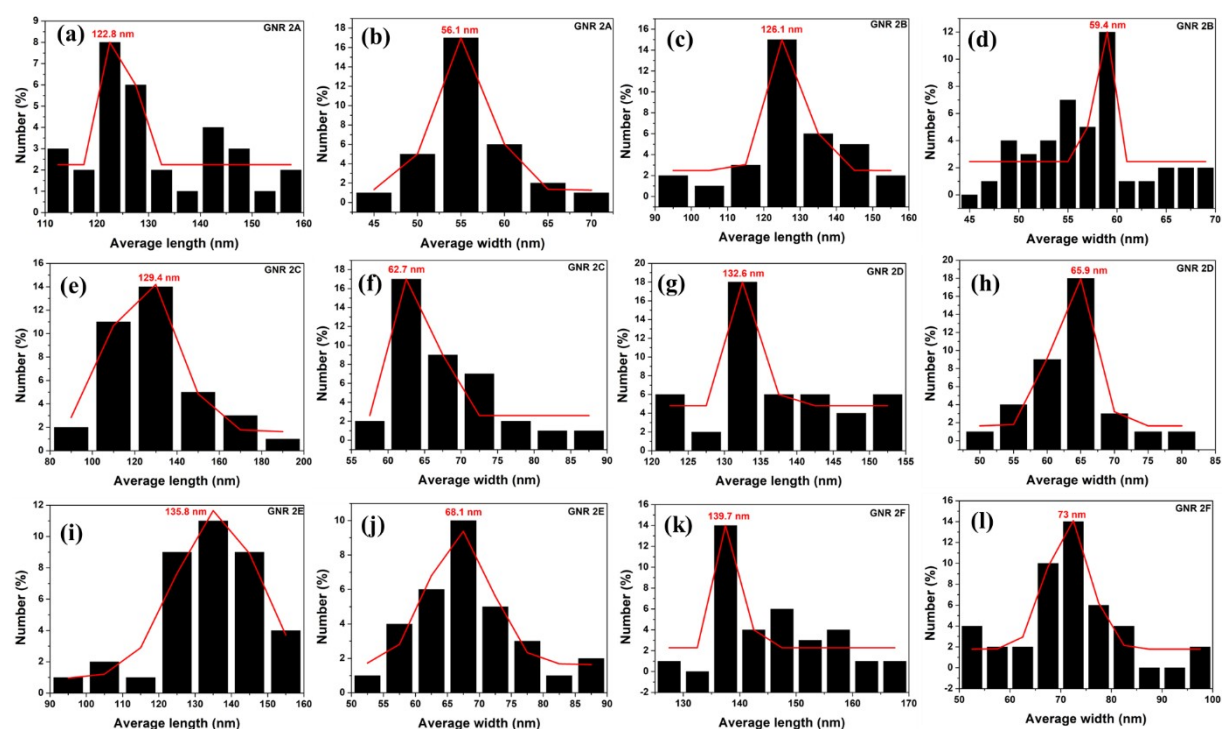


Figure S13: Average size plots of (a, b) GNR 2a, (c, d) GNR 2b, (e, f) GNR 2c, (g, h) GNR 2d, (i, j) GNR 2e, and (k, l) GNR 2f

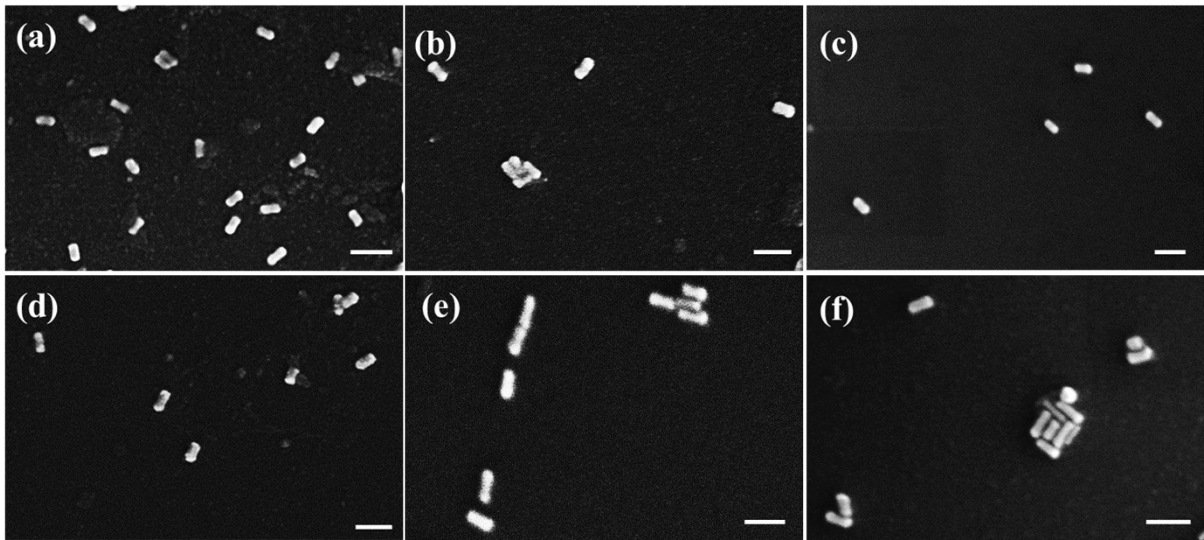


Figure S14: FE-SEM images of GNR 3 with different LBL assemblies (a) GNR 3a, (b) GNR 3b, (c) GNR 3c, (d) GNR 3d, (e) GNR 3e, and (f) GNR 3f and the scale bar is 200 nm

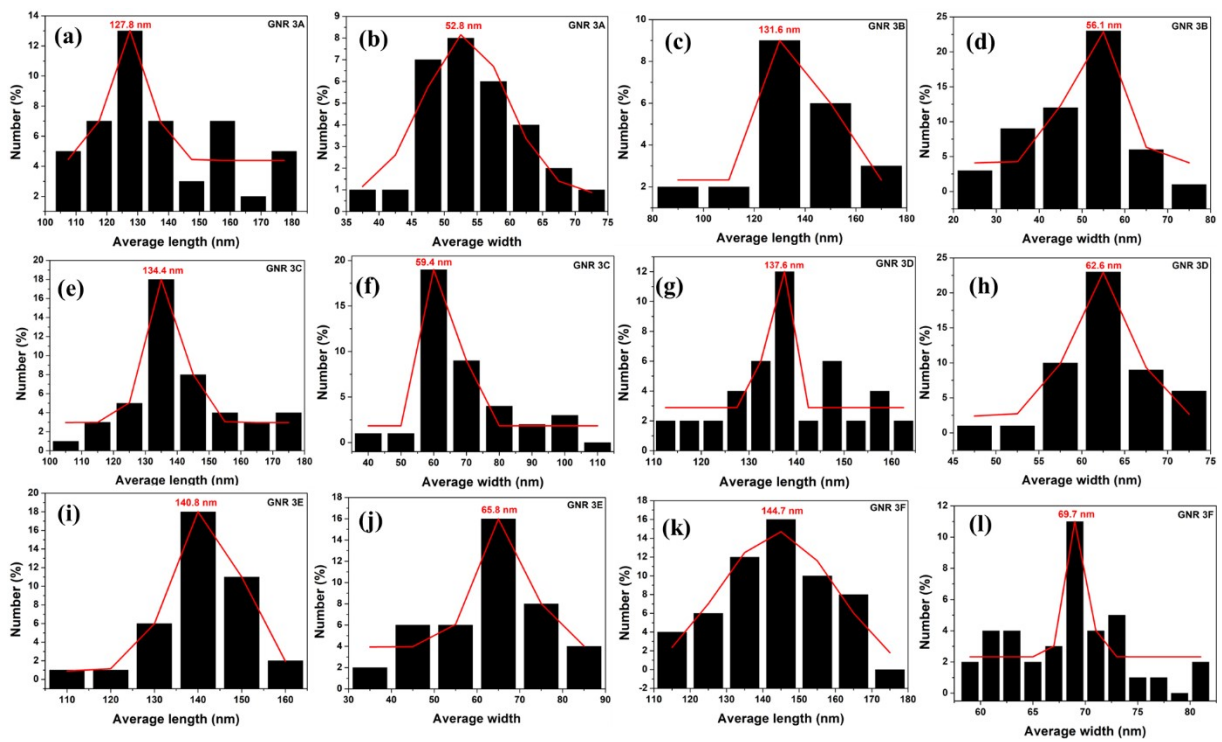


Figure S15: Average size plots of (a, b) GNR 3a, (c, d) GNR 3b, (e, f) GNR 3c, (g, h) GNR 3d, (i, j) GNR 3e, and (k, l) GNR 3f

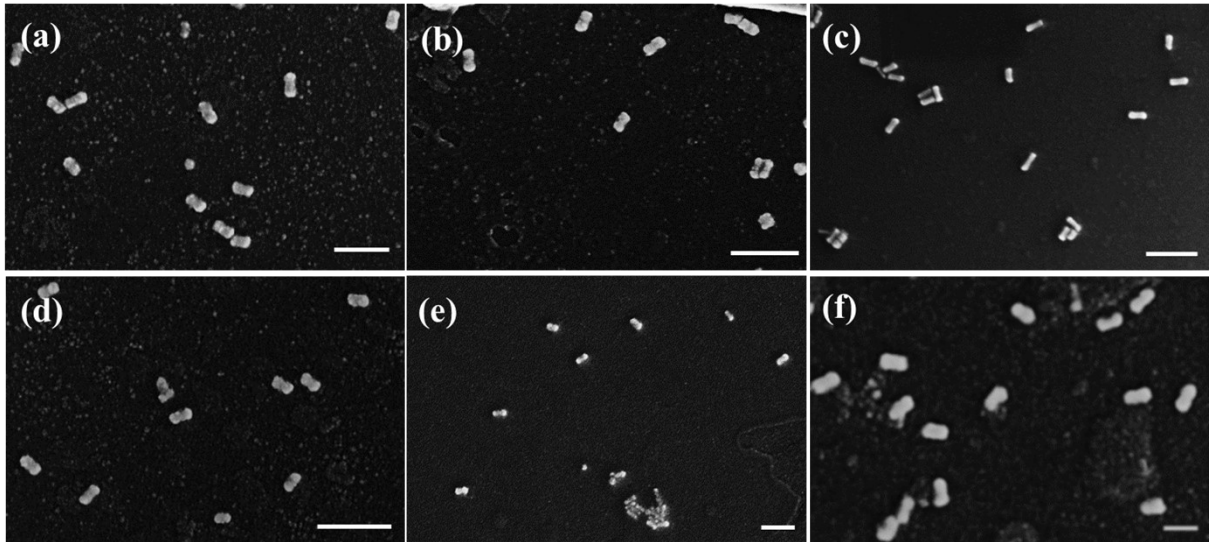


Figure S16: FE-SEM images of GNR 4 with different LBL assemblies (a) GNR 4a, (b) GNR 4b, (c) GNR 4c, (d) GNR 4d, (e) GNR 4e, and (f) GNR 4f and the scale bar is 400 nm

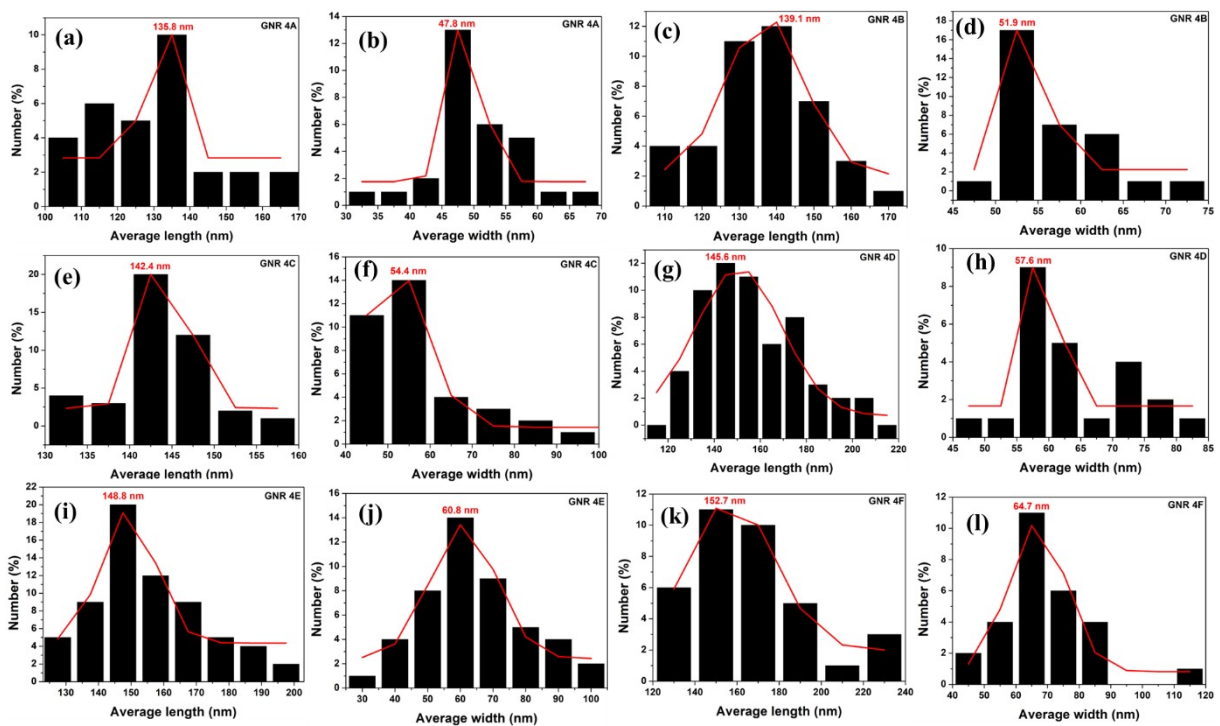


Figure S17: Average size plots of (a, b) GNR 4a, (c, d) GNR 4b, (e, f) GNR 4c, (g, h) GNR 4d, (i, j) GNR 4e, and (k, l) GNR 4f

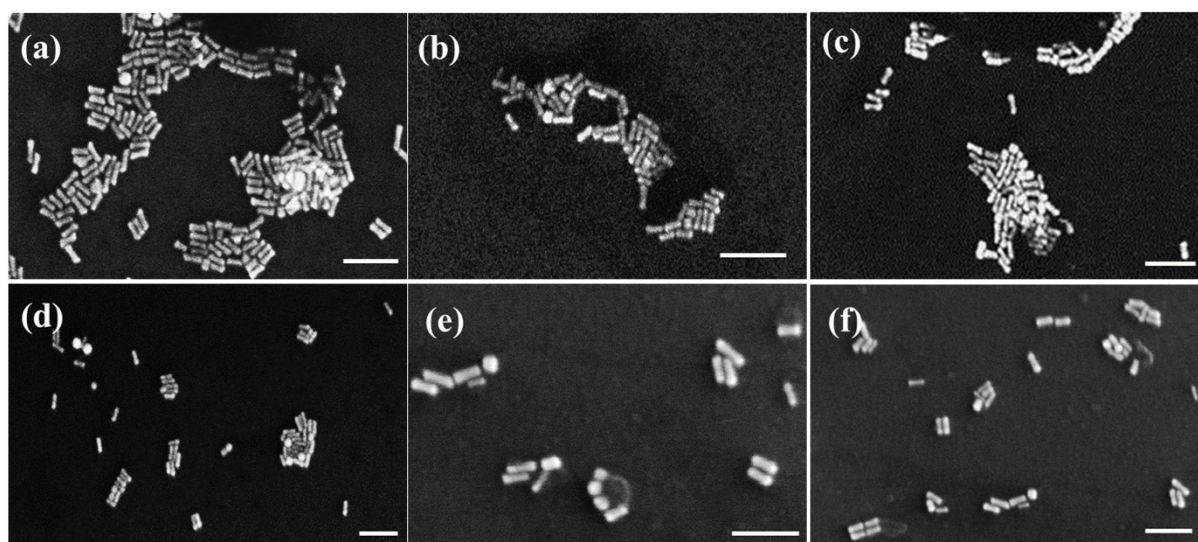


Figure S18: FE-SEM images of GNR 5 with different LBL assemblies (a) GNR 5a, (b) GNR 5b, (c) GNR 5c, (d) GNR 5d, (e) GNR 5e, and (f) GNR 5f and the scale bar is 400 nm

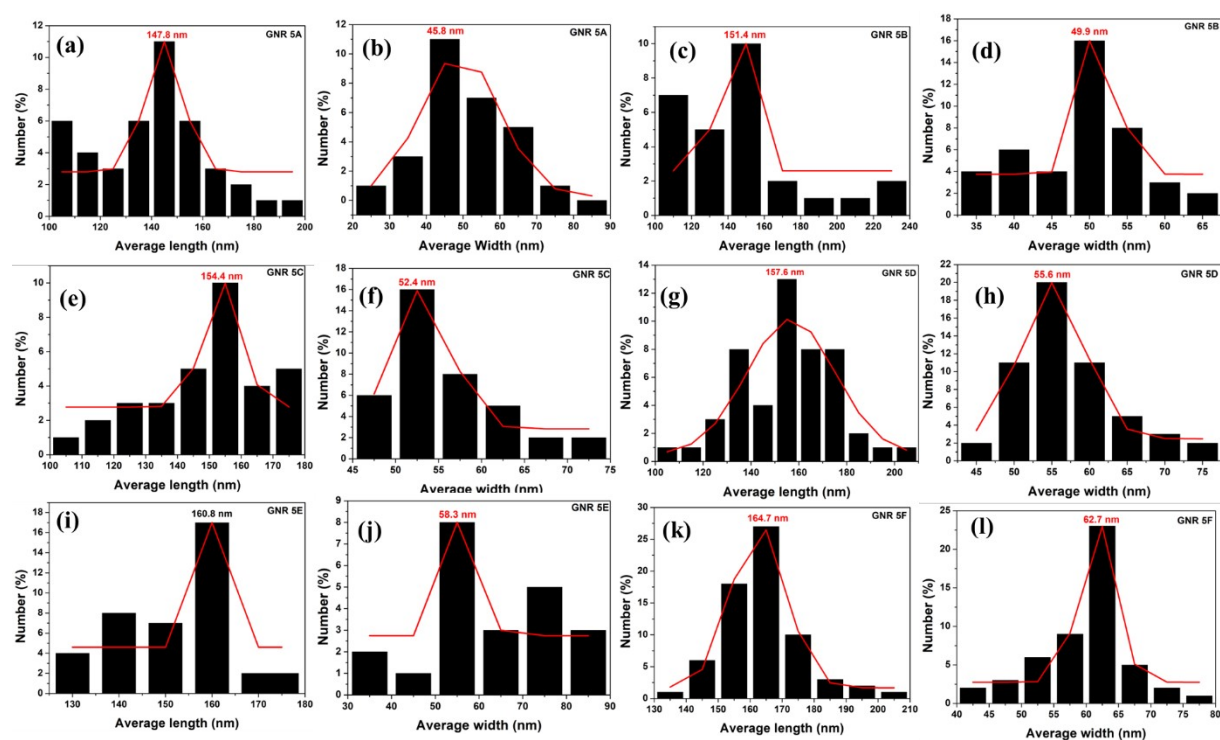


Figure S19: Average size plots of (a, b) GNR 5a, (c, d) GNR 5b, (e, f) GNR 5c, (g, h) GNR 5d, (i, j) GNR 5e, and (k, l) GNR 5f

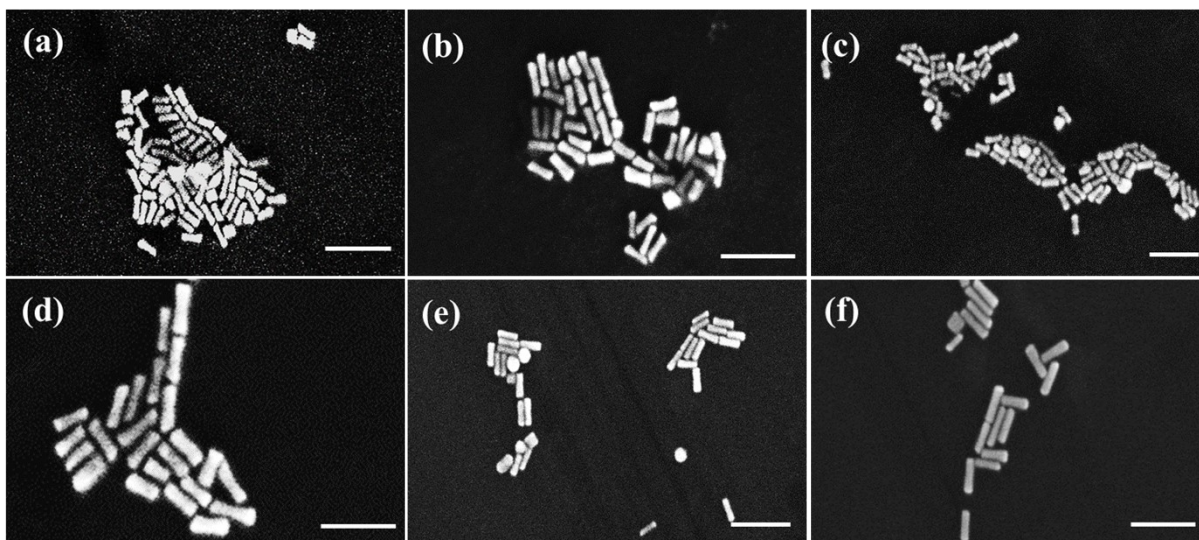


Figure S20: FE-SEM images of GNR 6 with different LBL assemblies (a) GNR 6a, (b) GNR 6b, (c) GNR 6c, (d) GNR 6d, (e) GNR 6e, and (f) GNR 6f and the scale bar is 400 nm

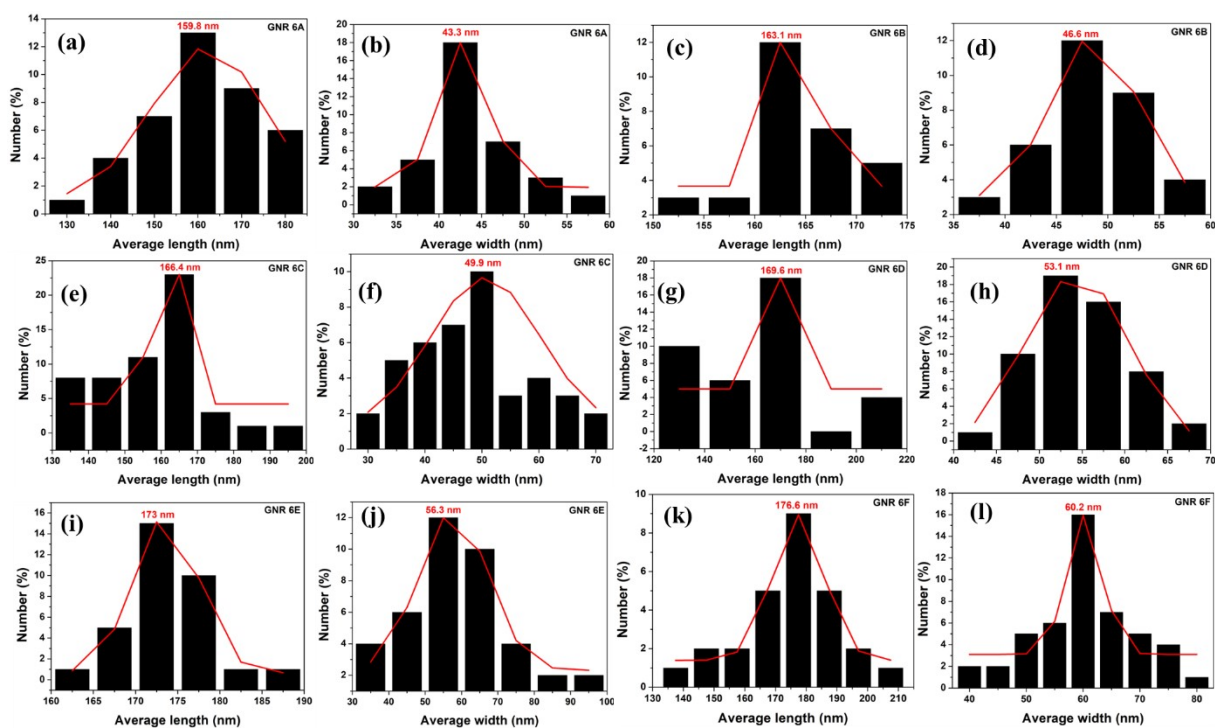


Figure S21: Average size plots of (a, b) GNR 6a, (c, d) GNR 6b, (e, f) GNR 6c, (g, h) GNR 6d, (i, j) GNR 6e, and (k, l) GNR 6f

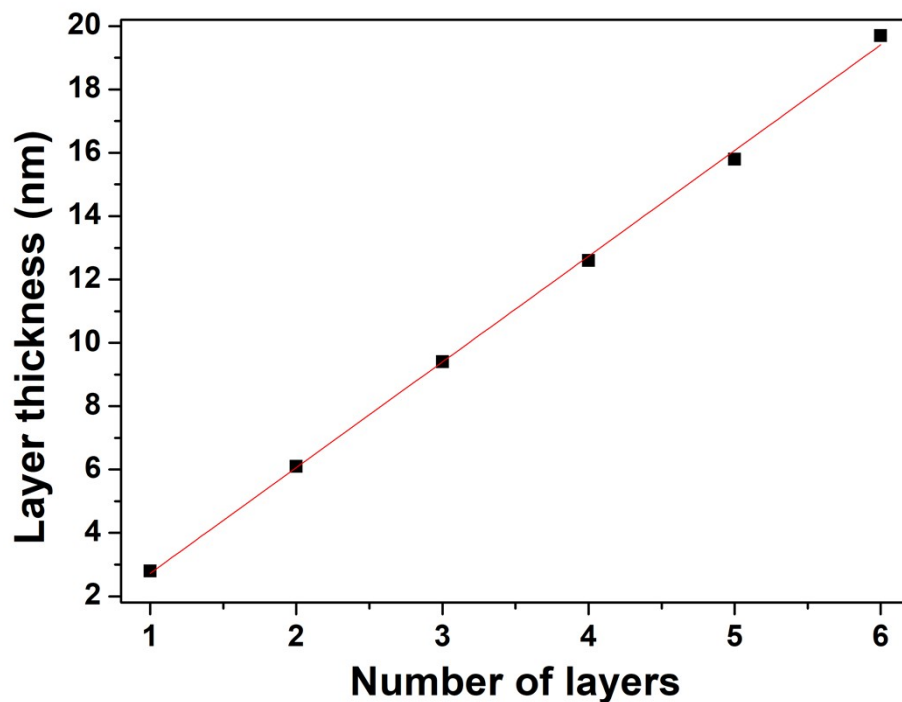


Figure S22: plot showing increase in average layer thickness with number of layers with GNR 4

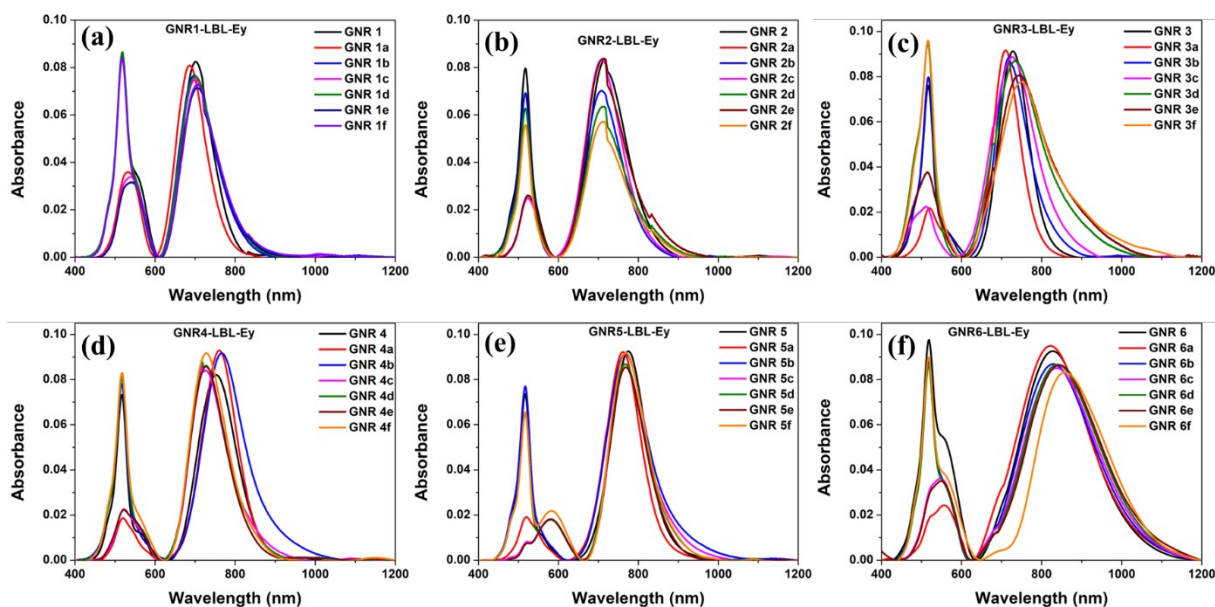


Figure S23: Extinction spectra of Ey conjugated GNR-LBL (a) GNR 1a-1f, (b) GNR 2a-2f, (c) GNR 3a-3f, (d) GNR 5a-5f, and (e) GNR 6a-6f

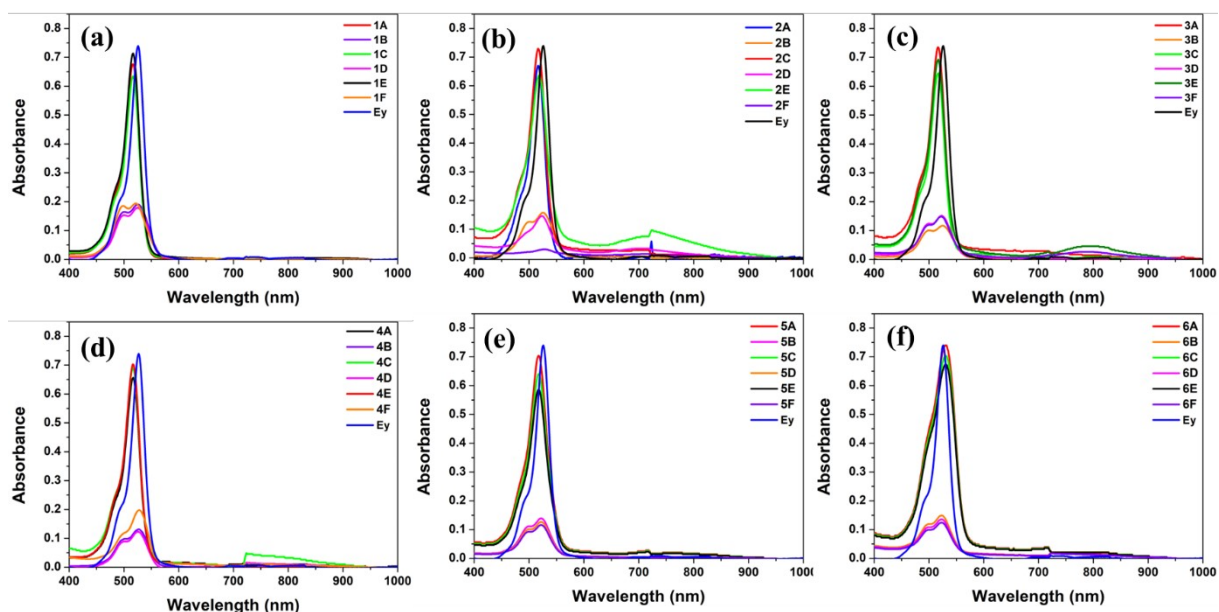


Figure S24: Extinction spectra of supernatants after EY conjugated (a) GNR 1a-1f, (b) GNR 2a-2f, (c) GNR 3a-3f, (d) GNR 4a-4f, (e) GNR 5a-5f and (f) GNR 6a-6f. In GNRs with outer layer as PSS, the supernatant absorbance is almost equal to the added EY absorbance and for that of PAH layers supernatant absorbance was very less indicating that EY got conjugated.

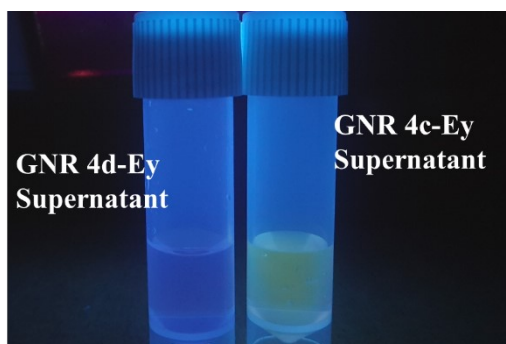


Figure S25: A representative photograph of supernatants under UV irradiation after final wash. We observed that in case of PSS as outer layer, there was a bright green emission similar to that of EY proving there is very less or no EY in the pellet. On the other hand, we do not observe any fluorescence in the supernatant of GNR-4d-Ey, where the outer layer is PAH indicating that most of the EY is present in the pellet.

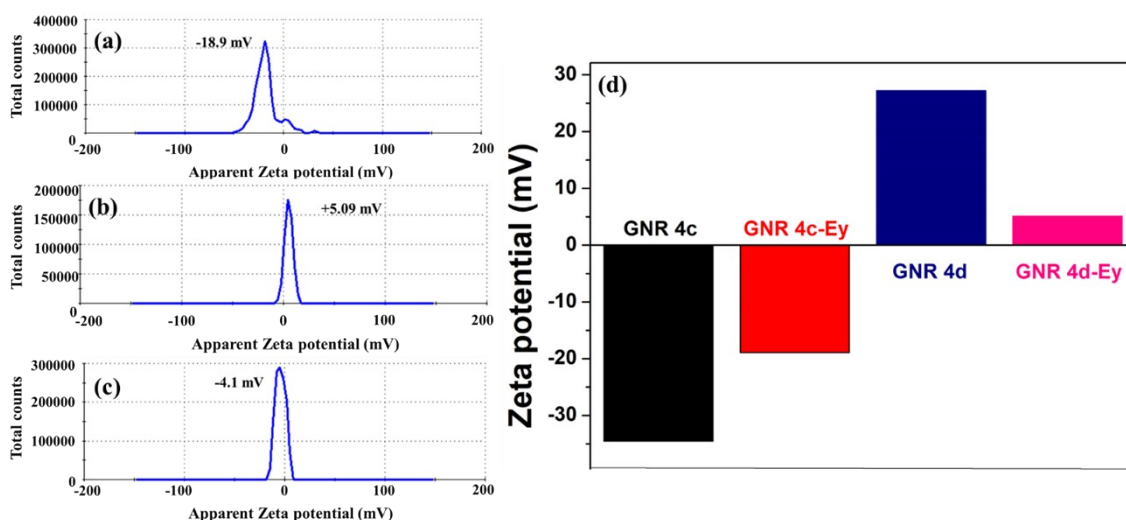


Figure S26: Zeta potential values of (a) GNR 4c-Ey, (b) GNR 4d-Ey, (c) Eosin Y, and (d) a representative histogram showing zeta change on GNR 4c and GNR 4d before and after Ey conjugation.

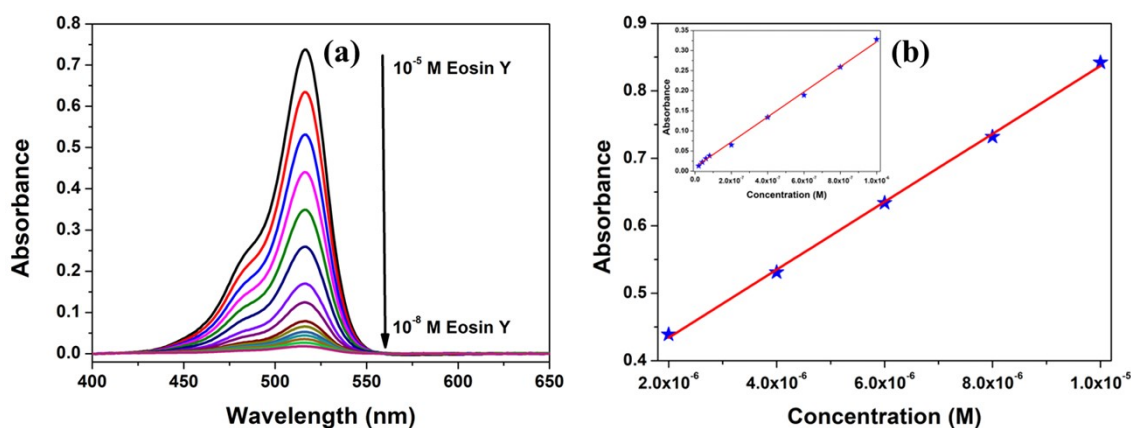


Figure S27: (a) is the absorbance spectra of Ey from 10 μM to 10 nM and (b) is calibration curve of Ey at higher and the inset shows the calibration curve in lower concentration range.

Calculation S1: Calculation of Number density

Number density of SiNPs:

Average size of SiNPs = 120 nm diameter = 60 nm radius = 60×10^{-7} cm

Density of TEOS = 0.933 g/mL or 0.94 g/cm³

Mass of Si precursor = Molecular weight \times Molarity \times volume/1000

$$= 208.33 \times 4.47 \text{ M} \times 50 \text{ mL}/1000$$

$$= 4.65 \text{ g}$$

Total Volume = mass/density

$$= 4.65\text{g} / 0.94\text{ g cm}^{-3}$$

$$= 4.94\text{ cm}^3$$

Total Volume occupied = $4/3 \pi r^3$

$$= 4/3 \times 3.14 \times (60 \times 10^{-7})^3$$

$$= 9.04 \times 10^{-16}\text{ cm}^3$$

Number of particles = Total volume/volume of each particle

$$= 4.94 / 9.04 \times 10^{-16}$$

$$= 5 \times 10^{15}\text{ particles/mL}$$

Number density of GNRs:

Average length of GNRs = 133 nm; width = 45 nm radius = $22.5 \times 10^{-7}\text{ cm}$

Density of gold salt = 3.9 g/cm^3

Mass of Au precursor = Molecular weight \times Molarity \times volume/1000

$$= 293.83 \times 0.5 \times 10^{-3}\text{ M} \times 50\text{ mL}/1000$$

$$= 7.34 \times 10^{-3}\text{ g}$$

Total Volume = mass/density

$$= 7.34 \times 10^{-3} / 3.9\text{ g cm}^{-3}$$

$$= 1.88 \times 10^{-3}\text{ cm}^3$$

Total Volume occupied = $\pi r^2 h$

$$= 3.14 \times (22.5 \times 10^{-7})^2 \times 133 \times 10^{-7}$$

$$= 2.11 \times 10^{-16}\text{ cm}^3$$

Number of particles = Total volume/volume of each particle

$$= 1.88 \times 10^{-3}\text{ cm}^3 / 2.11 \times 10^{-16}\text{ cm}^3$$

$$= 9 \times 10^{12}\text{ particles/mL}$$

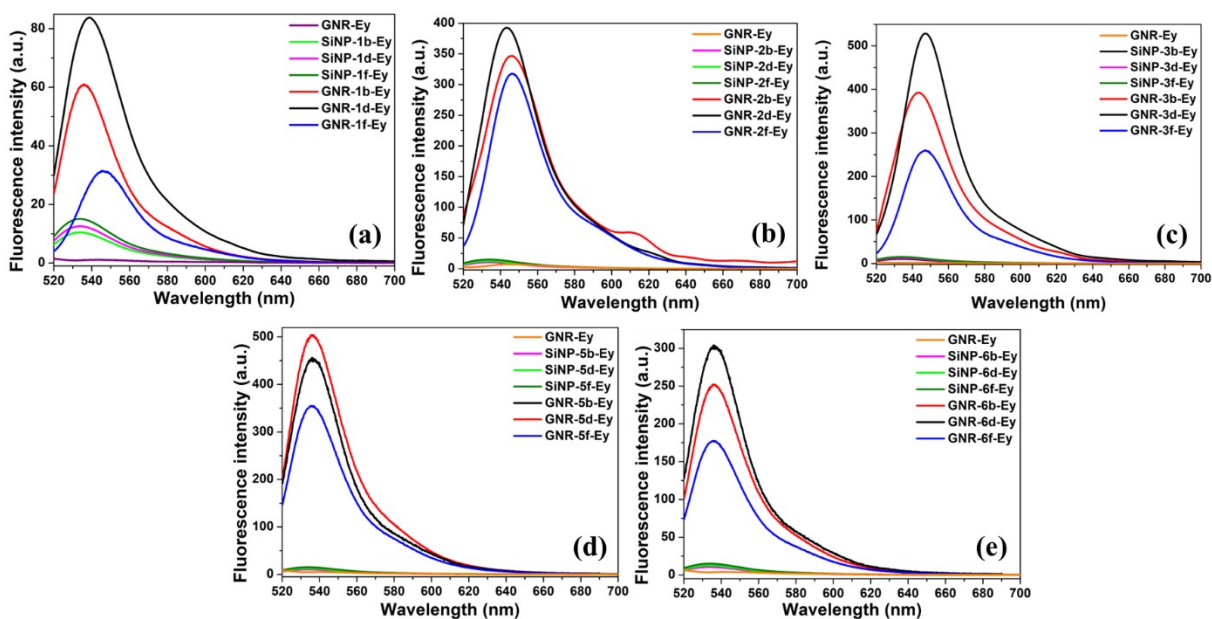


Figure S28: MEF studies of Ey adsorbed on (a) GNR 1b-1f, (b) GNR 2b-2f, (c) GNR 3b-3f, (d) GNR 5b-5f, and (e) GNR 6b-6f.

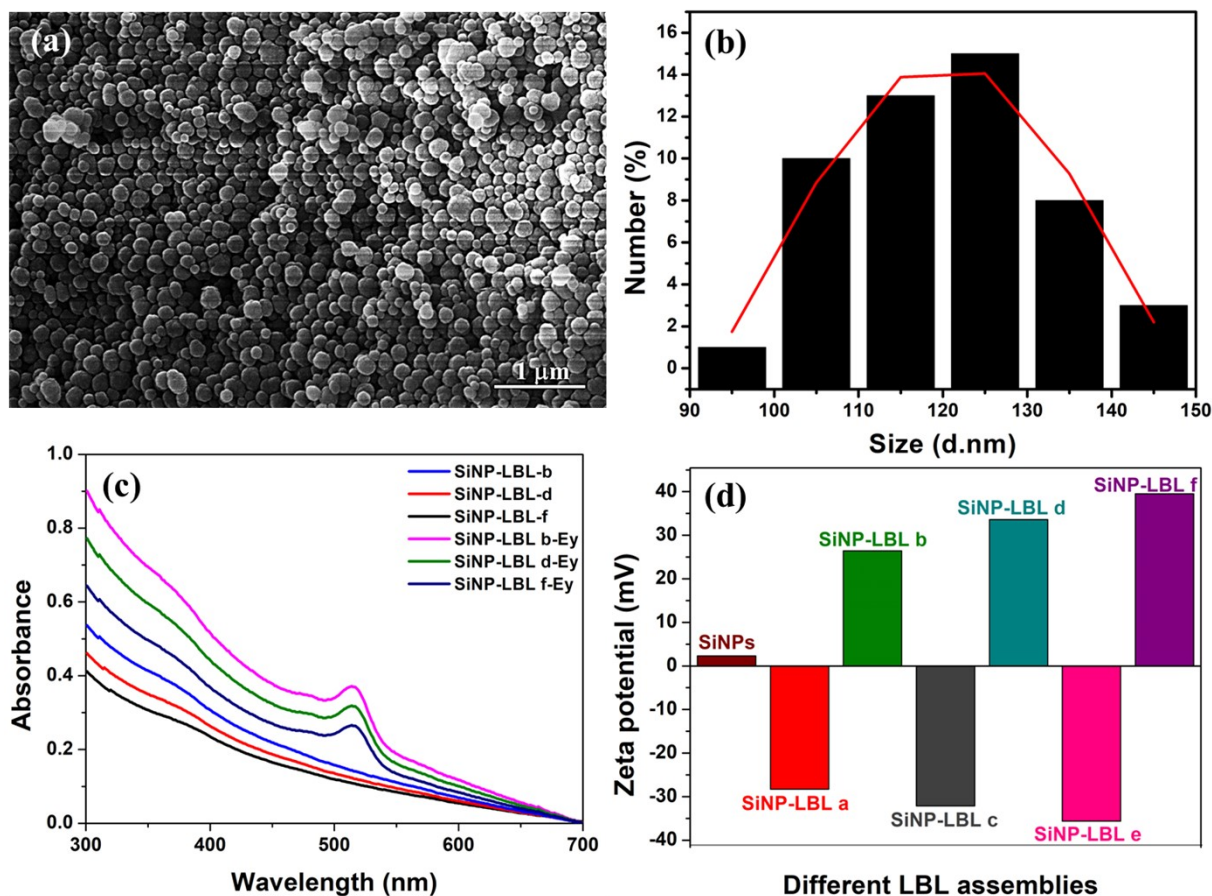


Figure S29: (a) FE-SEM image of SiNPs (b) Average size plots of SiNPs (c) Absorption spectra of SiNPs with PAH layers before and after Ey conjugation, and (d) Zeta potential values of SiNP a-f.

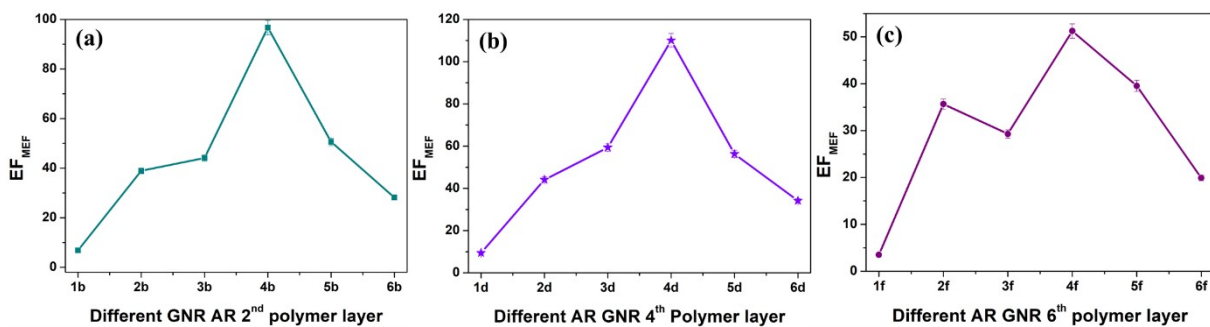


Figure S30: MEF EF of Ey adsorbed on (a) GNR 1b-6b, (b) GNR 1d-6d, and (c) GNR 1f-6f.

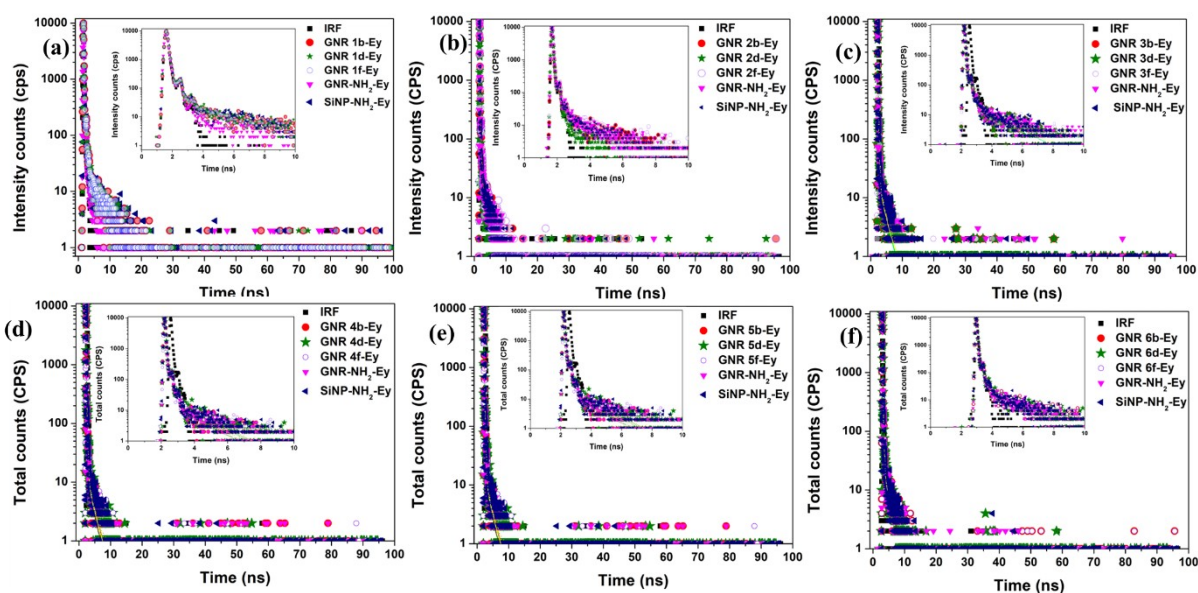


Figure S31: Life time plots of Ey adsorbed on (a) GNR 1a-1f, (b) GNR 2a-2f, (c) GNR 3a-3f, (d) GNR 5a-5f, and (e) GNR 6a-6f. Bare GNRs and SiNPs are ammine functionalized for the adsorption of Ey.

Table S2: Ey molecules lifetime values in water and after adsorption on to GNR 1 with PAH as outer layer

Sample	τ_1 (ns)	τ_2 (ns)	τ_3 (ns)	α_1 (%)	α_2 (%)	α_3 (%)	χ^2	Average life time(ns)
Ey in water	0.80	1.01	1.71	27.63	28.77	43.6	1.19	1.44
SiNP-NH ₂ -Ey	0.96	1.78	3.81	27.61	19.08	53.31	1.19	2.64
GNR1-Ey	0.17	0.82	1.02	10.01	39.92	50.06	1.17	0.85
GNR 1b-Ey	0.98	1.07	1.51	30.28	32.14	37.58	1.06	1.21
GNR 1d-Ey	0.82	1.02	1.11	28.44	49.55	22.01	1.18	0.99
GNR 1f-Ey	0.98	1.09	1.38	35.23	41.08	23.69	1.18	1.12

Table S3: Ey molecules lifetime values in water and after adsorption on to GNR 2 with PAH as outer layer

Sample	τ_1 (ns)	τ_2 (ns)	τ_3 (ns)	α_1 (%)	α_2 (%)	α_3 (%)	χ^2	Average life time(ns)
Ey in water	0.80	1.01	1.71	27.63	28.77	43.6	1.19	1.44
SiNP-NH ₂ -Ey	0.96	1.78	3.81	27.61	19.08	53.31	1.19	2.64
GNR 2-Ey	0.65	0.93	1.01	39.98	49.75	10.02	1.10	0.82
GNR 2b-Ey	0.98	1.27	1.45	51.83	16.69	31.48	1.2	1.18
GNR 2d-Ey	0.81	0.96	1.25	37.63	30.46	31.66	1.04	0.99
GNR 2f-Ey	0.86	0.95	1.25	25.08	24.98	49.9	1.01	1.08

Table S4: Ey molecules lifetime values in water and after adsorption on to GNR 3 with PAH as outer layer

Sample	τ_1 (ns)	τ_2 (ns)	τ_3 (ns)	α_1 (%)	α_2 (%)	α_3 (%)	χ^2	Average life time(ns)
Ey in water	0.80	1.01	1.71	27.63	28.77	43.6	1.19	1.44
SiNP-NH ₂ -Ey	0.96	1.78	3.81	27.61	19.08	53.31	1.19	2.64
GNR 3-Ey	0.59	0.92	1.08	36.01	49.97	14.02	1.16	0.83
GNR 3b-Ey	0.89	1.09	1.41	48.17	47.97	3.86	1.16	1.02
GNR 3d-Ey	0.66	0.81	1.10	15.05	51.35	33.61	1.11	0.89
GNR 3f-Ey	0.86	1.01	1.36	29.44	39.8	30.75	1.16	1.07

Table S5: Ey molecules lifetime values in water and after adsorption on to GNR 4 with PAH as outer layer

Sample	τ_1 (ns)	τ_2 (ns)	τ_3 (ns)	α_1 (%)	α_2 (%)	α_3 (%)	χ^2	Average life time(ns)
Ey in water	0.80	1.01	1.71	27.63	28.77	43.6	1.19	1.44
SiNP-NH ₂ -Ey	0.96	1.78	3.81	27.61	19.08	53.31	1.19	2.64
GNR 4-Ey	0.79	0.83	1.09	37.81	47.79	13.57	1.18	0.84
GNR 4b-Ey	0.86	1.01	1.22	26.81	50.19	23.01	1.16	1.02
GNR 4d-Ey	0.62	0.70	1.17	64.32	23.8	11.89	1.13	0.71
GNR 4f-Ey	0.88	1.01	1.36	49.41	31.09	19.5	1.14	1.02

Table S6: Ey molecules lifetime values in water and after adsorption on to GNR 5 with PAH as outer layer

Sample	τ_1 (ns)	τ_2 (ns)	τ_3 (ns)	α_1 (%)	α_2 (%)	α_3 (%)	χ^2	Average life time(ns)
Ey in water	0.80	1.01	1.71	27.63	28.77	43.6	1.19	1.44
SiNP-NH ₂ -Ey	0.96	1.78	3.81	27.61	19.08	53.31	1.19	2.64
GNR 5-Ey	0.46	0.96	1.08	30.66	40.03	29.32	1.14	0.84
GNR 5b-Ey	0.94	1.04	1.54	48.76	34.41	16.82	1.05	1.07
GNR 5d-Ey	0.82	0.92	1.06	19.94	30.03	50.03	1.13	0.94
GNR 5f-Ey	0.89	1.02	1.34	33.51	44.78	21.72	0.99	1.04

Table S7: Ey molecules lifetime values in water and after adsorption on to GNR 6 with PAH as outer layer

Sample	τ_1 (ns)	τ_2 (ns)	τ_3 (ns)	α_1 (%)	α_2 (%)	α_3 (%)	χ^2	Average life time(ns)
Ey in water	0.80	1.01	1.71	27.63	28.77	43.6	1.19	1.44
SiNP-NH ₂ -Ey	0.96	1.78	3.81	27.61	19.08	53.31	1.19	2.64
GNR 6-Ey	0.45	0.85	1.09	28.17	30.02	41.81	1.06	0.84
GNR 6b-Ey	0.89	1.29	1.57	31.33	19.01	28.99	1.04	0.99
GNR 6d-Ey	0.87	1.02	1.22	50.01	46.85	3.15	1.04	0.95
GNR 6f-Ey	0.89	0.94	1.24	19.87	49.8	30.33	1.14	1.02

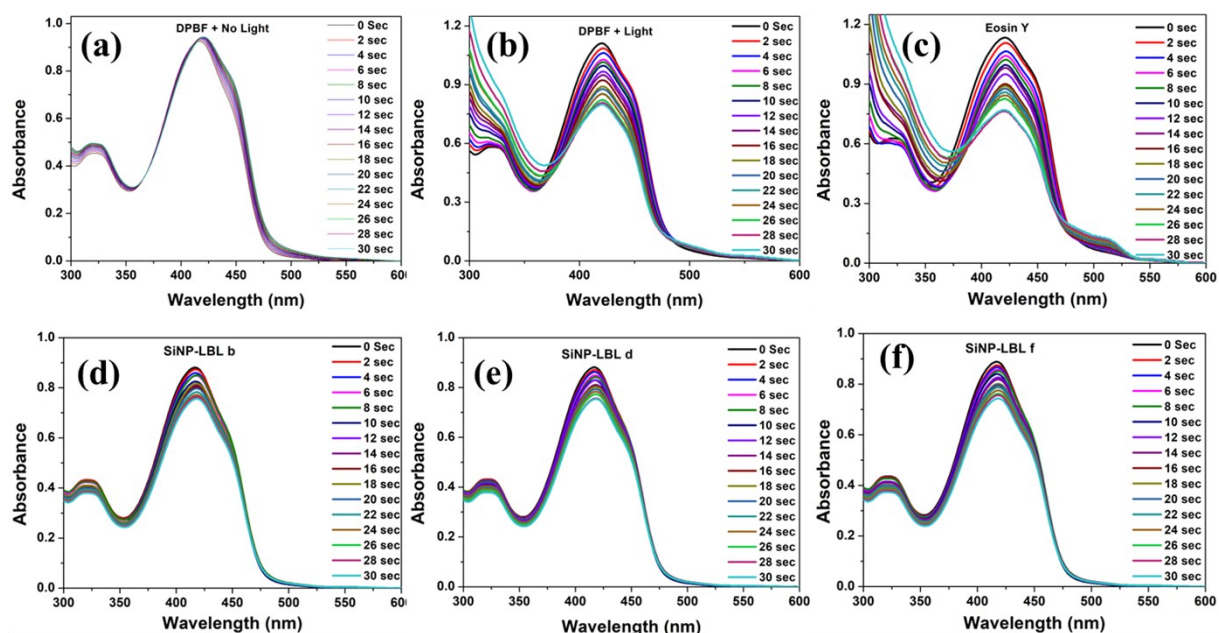


Figure S32: Blank study showing DPBF degradation (a) in the absence of light, (b) presence of light, (c) in presence of 1 μ M Ey, (d) SiNPs-LBL b-Ey, (e) SiNPs-LBL d-Ey, and (f) SiNPs-LBL f-Ey under 35 mW cm⁻² white light irradiation. 1 μ M Ey was used for (d) to (f).

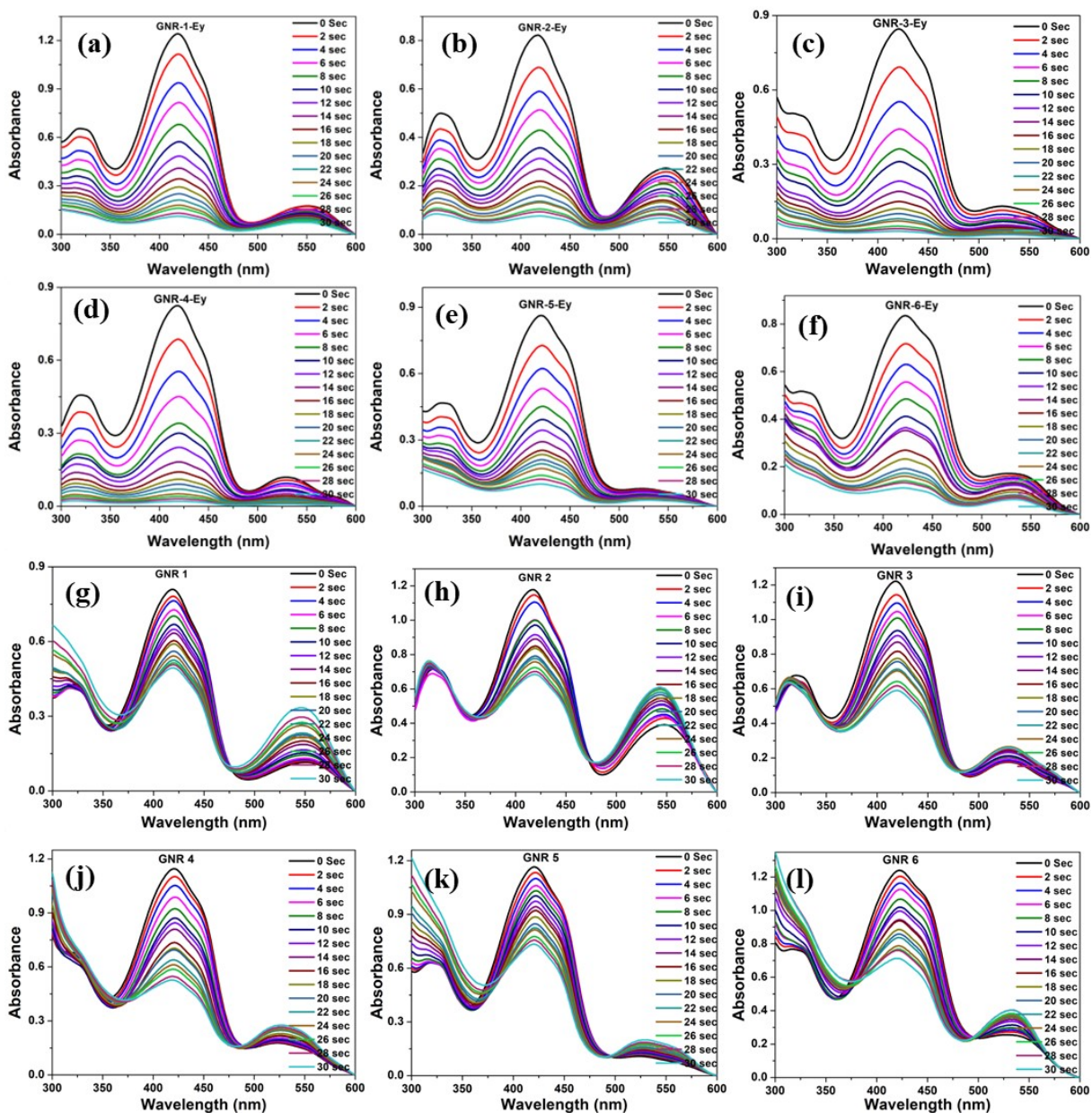


Figure S33: Degradation of 50 μM DPBF on (a) GNR 1-Ey, (b) GNR 2-Ey, (c) GNR 3-Ey, (d) GNR 4-Ey, (e) GNR 5-Ey, (f) GNR 6-Ey, (g) GNR-1-DPBF, (h) GNR-2-DPBF, (i) GNR-3-DPBF, (j) GNR-4-DPBF, (k) GNR-5-DPBF, and (l) GNR-6-DPBF, under 35 mW cm^{-2} white light irradiation

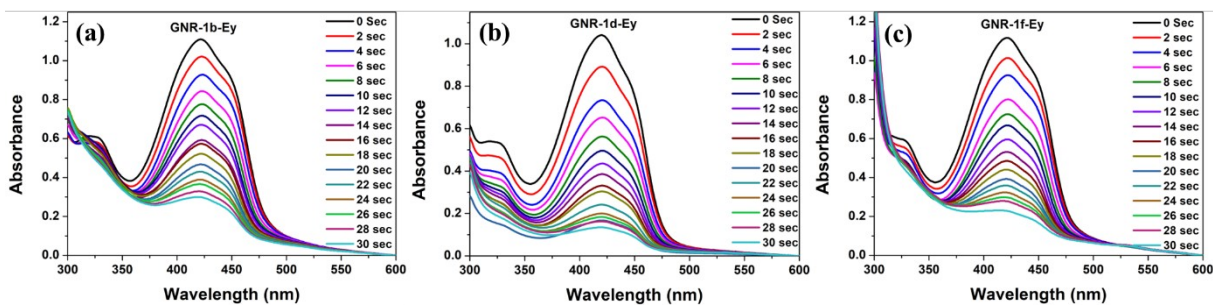


Figure S34: Degradation of 50 μM DPBF on (a) GNR 1b-Ey, (b) GNR 1d-Ey, and (c) GNR 1f-Ey under 35 mW cm^{-2} white light irradiation.

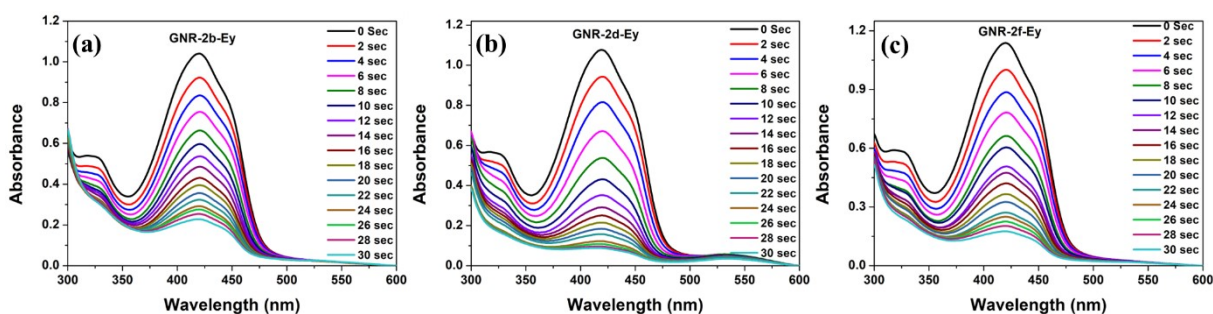


Figure S35: Degradation of 50 μM DPBF on (a) GNR 2b-Ey, (b) GNR 2d-Ey, and (c) GNR 2f-Ey under 35 mW cm^{-2} white light irradiation

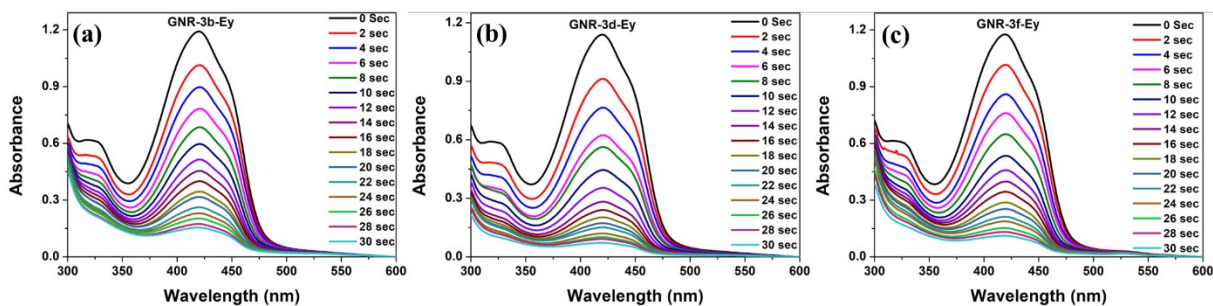


Figure S36: Degradation of 50 μM DPBF on (a) GNR 3b-Ey, (b) GNR 3d-Ey, and (c) GNR 3f-Ey under 35 mW cm^{-2} white light irradiation

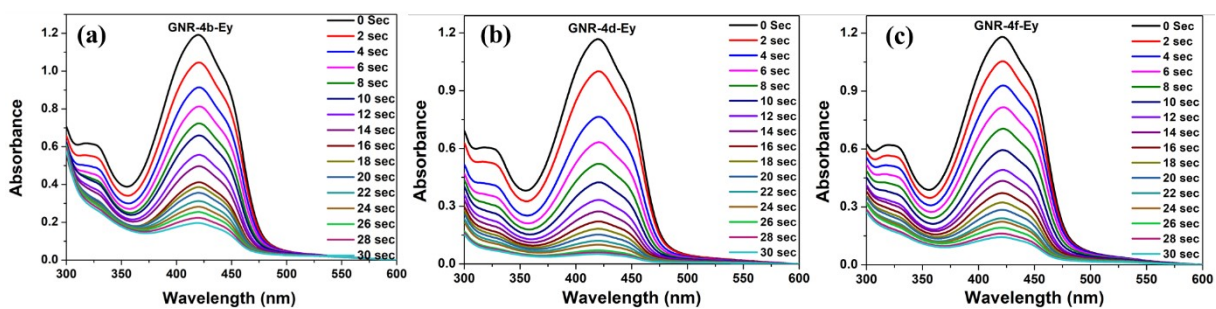


Figure S37: Degradation of 50 μM DPBF on (a) GNR 4b-Ey, (b) GNR 4d-Ey, and (c) GNR 4f-Ey under 35 mW cm^{-2} white light irradiation

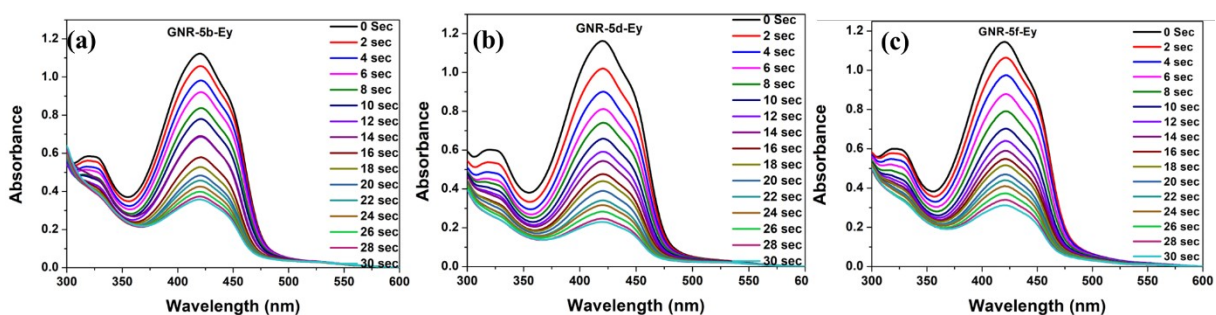


Figure S38: Degradation of 50 μM DPBF on (a) GNR 5b-Ey, (b) GNR 5d-Ey, and (c) GNR 5f-Ey under 35 mW cm^{-2} white light irradiation.

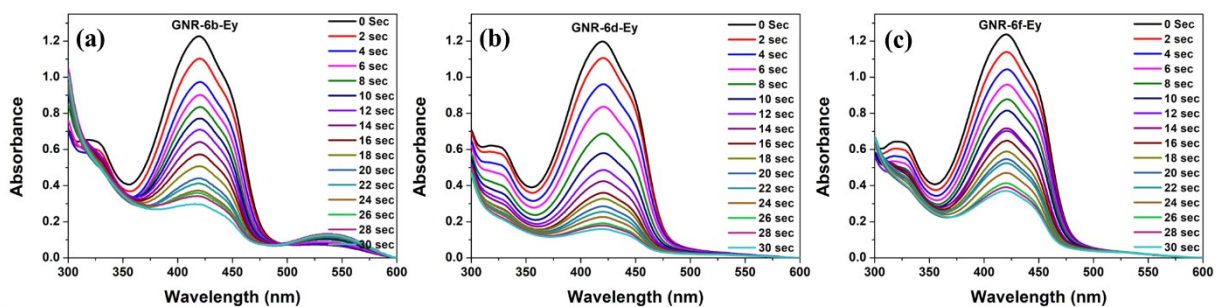


Figure S39: Degradation of 50 μM DPBF on (a) GNR 6b-Ey, (b) GNR 6d-Ey, and (c) GNR 6f-Ey under 35 mW cm^{-2} white light irradiation

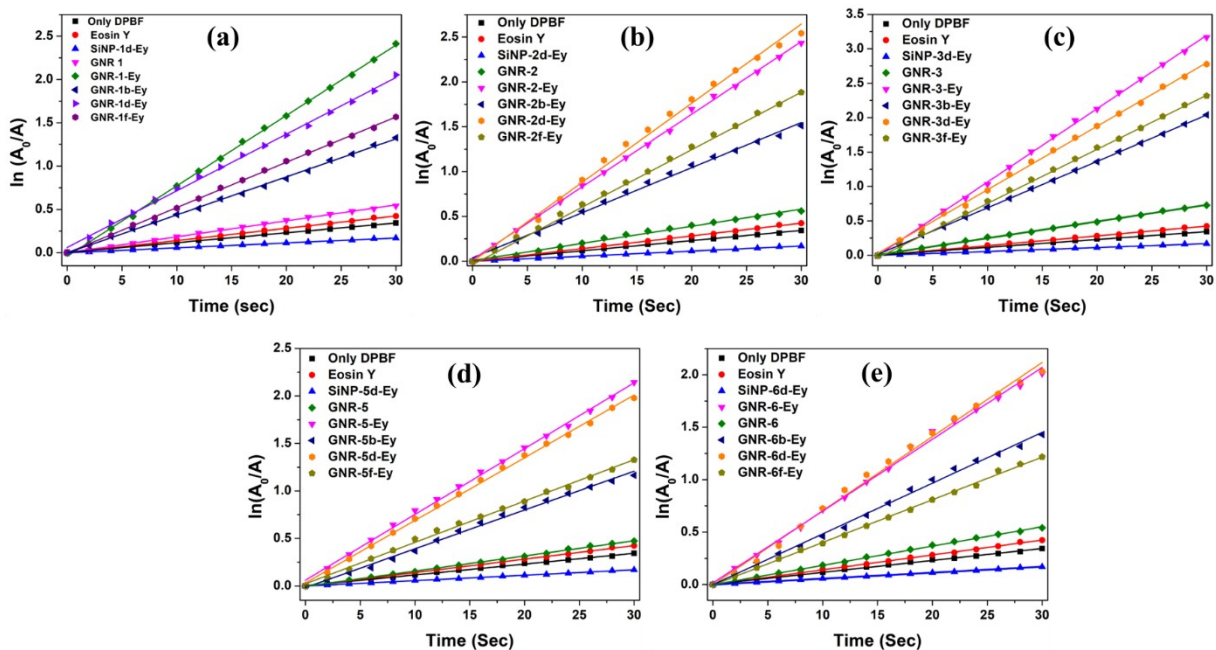


Figure S40: $\ln(A_0/A)$ plots depicting the degradation of 50 μM DPBF on (a) GNR 1a-Ey to 1f-Ey, (b) GNR 2a-Ey to 2f-Ey, (c) GNR 3a-Ey to 3f-Ey, (d) GNR 4a-Ey to 4f-Ey, (e) GNR 5a-Ey to 5f-Ey, and (f) GNR 6a-Ey to 6f-Ey under 35 mW cm^{-2} white light irradiation

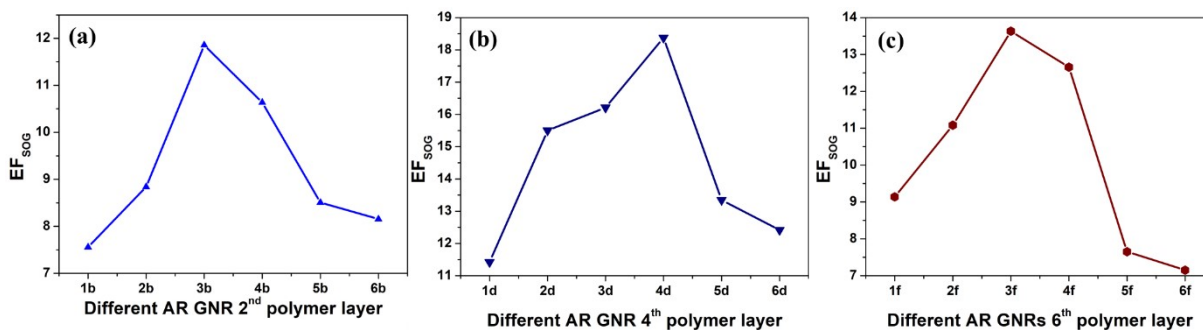


Figure S41: SOG EF of Ey adsorbed on (a) GNR 1b-6b, (b) GNR 1d-6d, (c) GNR 1f-6f.

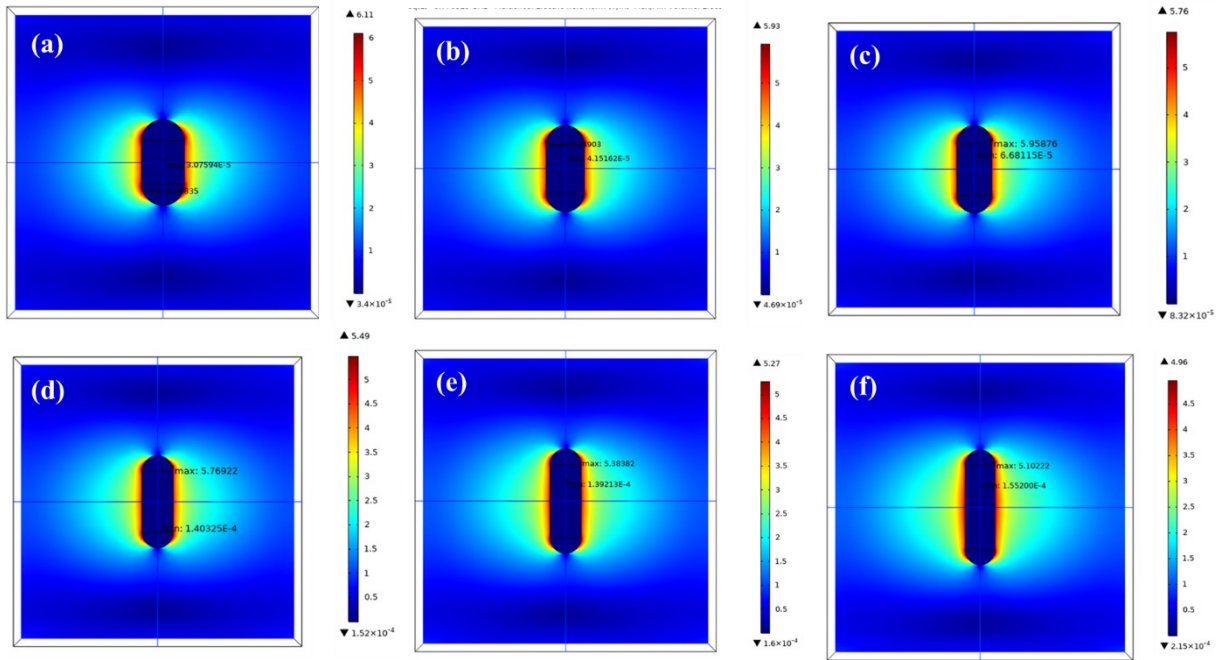


Figure S42: Theoretical Electromagnetic field maps for (a) GNR 1, (b) GNR 2, (c) GNR 3, (d) GNR 4, (e) GNR 5, and (f) GNR 6.

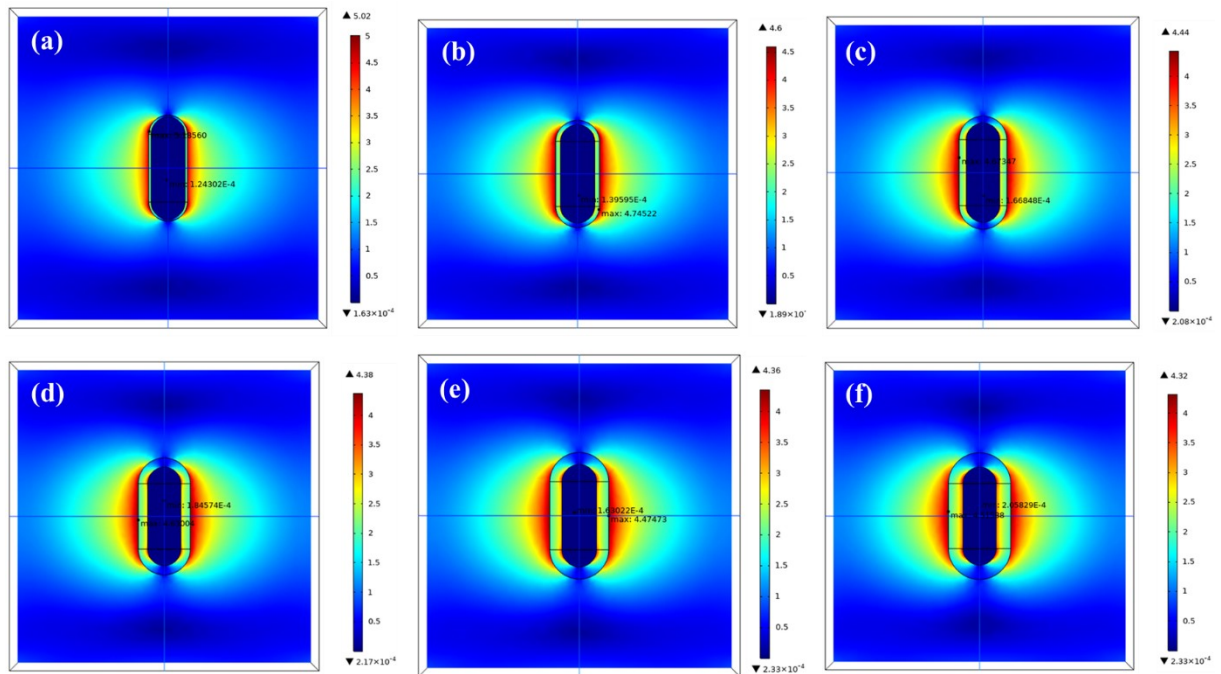


Figure S43: Theoretical Electromagnetic field maps for (a) GNR 4a, (b) GNR 4b, (c) GNR 4c, (d) GNR 4d, (e) GNR 4e, and (f) GNR 4f.

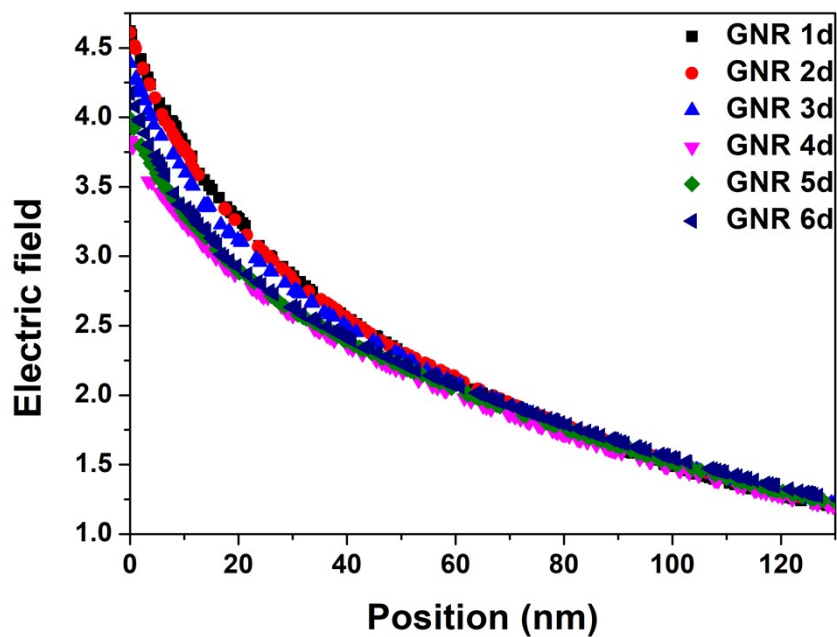


Figure S44: Decay length plot of GNR 1d-6d.

Decay length is calculated as $1/e$ of the initial value of the electric field.

For example: $1/e = 0.3678$ and the initial value of electric field for GNR 4d is 3.78 from Fig. S44. Therefore, the corresponding x value for the electric field in the y axis ($0.3678 \times 3.78 = 1.39$) is 107.7 nm. Therefore, the decay length of GNR 4d is 107.7 nm

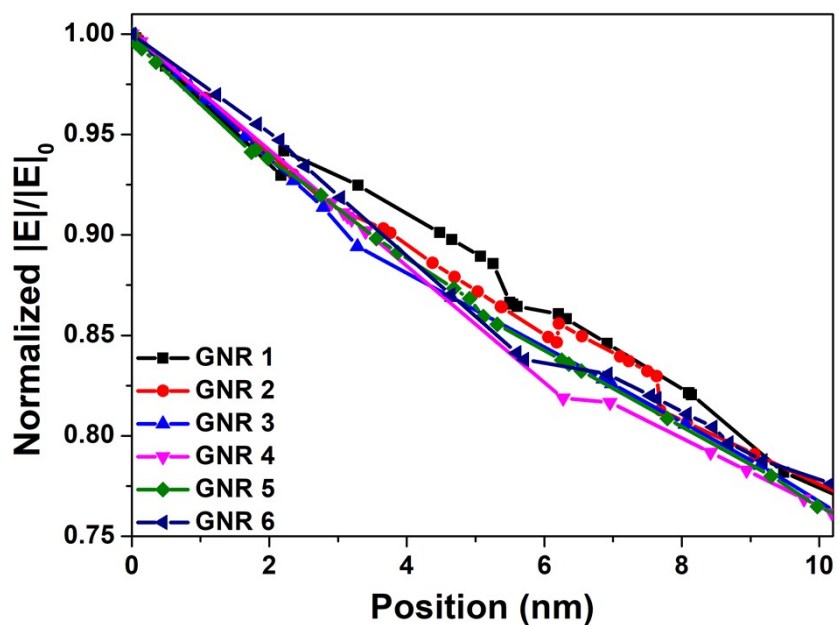


Figure S45: 1D line plot showing the normalized electric field damping as a function of distance for bare GNRs

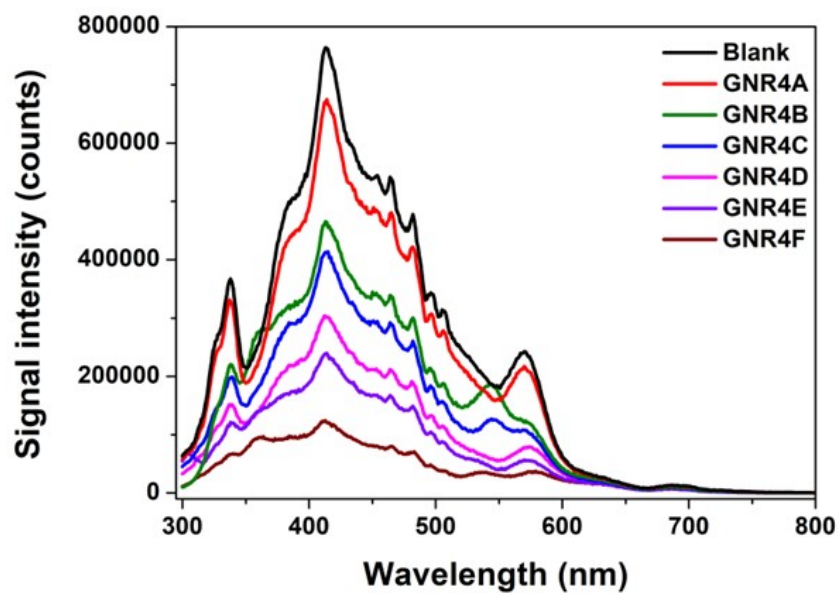


Figure S46: Experimental scattering values observed for GNR 4a-4f.

References:

1. S. S. Shafqat, A. A. Khan, M. N. Zafar, M. H. Alhaji, K. Sanaullah, S. R. Shafqat, S. Murtaza and S. C. Pang, *J. Mater. Res. Technol.*, 2019, 8, 385–395.
2. M. Bregnhøj, S. Rodal-Cedeira, I. Pastoriza-Santos and P. R. Ogilby, *J. Phys. Chem. C*, 2018, 122, 15625–15634.
3. N. Macia, V. Kabanov, M. Côté-Cyr and B. Heyne, *J. Phys. Chem. Lett.*, 2019, 10, 3654–3660.